Diversity in Complexation of $[Rh^I(cod)]^+$ and $[Ir^I(cod)]^+$ by Pyridine-Amine-Pyrrole Ligands

Bas de Bruin,[a] Reinout J. N. A. M. Kicken,[a] Nicolaas F. A. Suos,[a] Maurice P. J. Donners,[a] Carolien J. den Reijer,[a] Albertus J. Sandee,[a] René de Gelder,[a] Jan M. M. Smits,[a] Anton W. Gal,*[a] and Anton L. Spek[b]

Keywords: Rhodium / Iridium / N ligands / Coordination modes / Polymerizations

Complexation of $[Rh^I(cod)]^+$ and $[Ir^I(cod)]^+$ by the new pyridine-amine-pyrrole ligands Py–CH_2–N(R)–CH_2–Pyr–H (HL_R; R = H, Bzl, Bu) and the corresponding pyridine-amine-pyrrolate ligands $[Py–CH_2–N(R)–CH_2–Pyr]^-$ (L_R^-; R = H, Bzl, Bu, CH_2Py) has been investigated. The neutral ligands HL_R (R = H, Bu, Bzl) give $[(HL_R)M^I(cod)]^+$ (M = Rh, Ir) in which HL_R acts as a didentate ligand via the pyridine nitrogen (N_{Py}) and the amine nitrogen (N^R_{amine}). The crystal structures of $[(HL_H)M^I(cod)]PF_6$ (M = Rh: **[1]**PF_6 and M = Ir: **[2]**PF_6) have been determined. Deprotonation of $[(HL_R)M^I(cod)]^+$ (M = Rh, Ir; R = H, Bzl, Bu) results in the neutral complexes $[(L_R)M^I(cod)]$ (M = Rh, Ir) of the mono-anionic ligands L_R^- (R = H, Bzl, Bu). In square-planar $[(L_H)M^I(cod)]$ (M = Rh: **3**, M = Ir: **4**), L_H^- is didentate via N^H_{amine} and the pyrrolate nitrogen (N_{Pyr}). The X-ray structures of **3** and **4** reveal that in both cases the uncoordinated N_{Py} accepts a hydrogen bond from N^H_{amine}. The X-ray structures of $[(L_{Bzl})M^I(cod)]$ (M = Rh: **5**, M = Ir: **6**), show that L_{Bzl}^- is didentate via N_{amine} and N_{Pyr} for M = Rh and tridentate for M = Ir. In solution L_{Bzl}^- is tridentate for both M = Rh and M = Ir. The neutral complexes $[\{Py–CH_2–N(R)–CH_2–Pyr\}M^I(cod)]$ (M = Rh, Ir) cannot be oxidised selectively with H_2O_2. This is in marked contrast to the previously observed selective oxidation of the corresponding cationic complexes $[\{Py–CH_2–N(R)–CH_2–Py\}Rh^I(cod)]^+$. Rhodium complex **5** is an active catalyst for the stereoregular polymerisation of phenylacetylene, whereas iridium complex **6** is inactive.

Introduction

Multidentate N-donor ligands ("N_x" ligands) have thusfar found limited application in the organometallic chemistry of rhodium(I) and iridium(I). Interesting reactivity has, however, been reported for triazacyclononane,[1][2] trispyrazolylborate,[2] and pyridine-2,6-diimine[3] complexes. We recently described the fast and selective mono-oxygenation of $[Rh^I(cod)]^+$ to $[Rh^{III}(oxabicyclononadiyl)]^+$ with aqueous hydrogen peroxide.[4] In this reaction $[Rh^I(cod)]^+$ is stabilised by the neutral tridentate pyridine-amine-pyridine ligands Py−CH_2−N(R)−CH_2−Py (R = H, Bu, Bzl). As part of our investigation into the tolerance of the observed oxygenation to changes in the nitrogen donor ligands, we have prepared and characterised a series of neutral complexes $[\{Py−CH_2−N(R)−CH_2−Pyr\}M^I(cod)]$ (M = Rh, Ir). In these, $[M^I(cod)]^+$ is stabilised by the potentially tridentate pyridine-amine-pyrrolate ligands $[Py−CH_2−N(R)−CH_2−Pyr]^-$ ($[L_R]^-$; R = H, Bzl, Bu). The complexes were obtained by deprotonation of the cationic complexes $[\{Py−CH_2−N(R)−CH_2−Pyr−H\}M^I(cod)]^+$ which result from reaction of $[\{(cod)M^I(\mu\text{-}Cl)\}_2]$ (M = Rh, Ir) with the neutral didentate ligands Py−CH_2−N(R)−CH_2−Pyr−H (HL_R;R = H, Bu, Bzl).

[a] Department of Inorganic Chemistry, University of Nijmegen, Toernooiveld 1, NL-6525 ED Nijmegen, The Netherlands
Fax: (internat.) +31-24/ 355-3450
E-mail: gal@sci.kun.nl
[b] Department of Crystal and Structural Chemistry, Bijvoet Centre for Biomolecular Research, University of Utrecht

Results and Discussion

Synthesis of the Ligands HL_R

The neutral ligands HL_R (R = H, Bzl, Bu; see Figure 1) were prepared via the synthesis routes shown in Scheme 1.

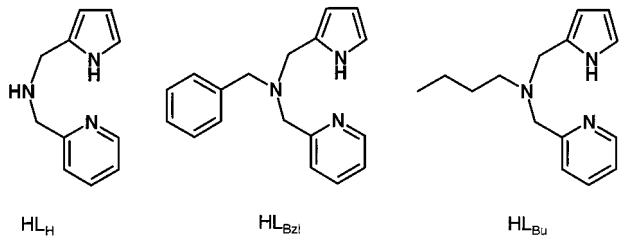

Figure 1. Pyridine-amine-pyrrole ligands HL_H, HL_{Bzl}, and HL_{Bu}

N-(2-pyridylmethyl)-*N*-(1*H*-2-pyrrolylmethyl)amine (HL_H) was prepared in two steps: condensation of 2-pyridylmethylamine and pyrrole-2-carboxaldehyde to the corresponding imine and subsequent reduction of the imine with $NaBH_4$. *N*-benzyl-*N*-(2-pyridylmethyl)-*N*-(1*H*-2-pyrrolylmethyl)-amine (HL_{Bzl}) and *N*-butyl-*N*-(2-pyridylmethyl)-*N*-(1*H*-2-pyrrolylmethyl)amine (HL_{Bu}) were prepared in three steps: *N*-benzyl-*N*-(1*H*-2-pyrrolylmethylidene)amine and *N*-butyl-*N*-(2-pyrrolylmethylidene)amine were obtained by condensation of pyrrole-2-carboxaldehyde with benzylamine and *n*-butylamine, respectively. The imines were reduced to the corresponding amines with $NaBH_4$. Alkylation of the amines with 2-picolyl chloride in a suspension of Na_2CO_3 in CH_3CN gave HL_{Bzl} and HL_{Bu}, respectively.

  1434−1948/99/0909−1581 $ 17.50+.50/0

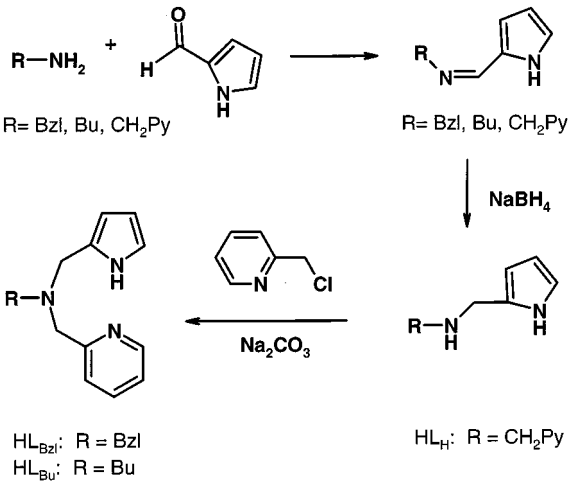

Scheme 1. Synthesis of the ligands HL_H, HL_{Bzl}, and HL_{Bu}

Structure of HL_H

Colourless crystals of compound HL_H were obtained by crystallisation from a hot saturated toluene solution. The structure of HL_H was determined by single-crystal X-ray diffraction (Figure 2).

In the crystal, the enantiomers (*R*) and (*S*) of HL_H occur as hydrogen-bridged dimers (*R*,*R*) and (*S*,*S*) in which the pyrrole N−H (N_{Pyr}−H) acts as a hydrogen bond donor, and the amine nitrogen (N_{amine}) as a hydrogen bond acceptor [N_{Pyr}−N_{amine} distance: 3.02(1) Å, H−N_{amine} distance: 2.09(6) Å, N_{Pyr}−H−N_{amine} angle: 169(4)°]. Selected bond lengths and angles are given in Tables 1 and 2. Crystallographic data are given in Table 4.

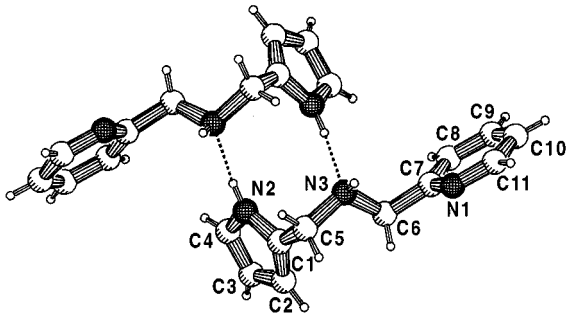

Figure 2. X-ray structure of ligand HL_H [the crystal contains the dimers (*R*,*R*) and (*S*,*S*) of the enantiomers (*R*) and (*S*); only (*R*,*R*) is shown]

Complexation of $[Rh^I(cod)]^+$ and $[Ir^I(cod)]^+$ by HL_H

Reaction of HL_H with $[\{(cod)Rh(\mu\text{-}Cl)\}_2]$ in methanol, followed by addition of an excess of NH_4PF_6, resulted in precipitation of $[(HL_H)Rh^I(cod)]PF_6$, [**1**]PF_6. Crystals of [**1**]PF_6 were obtained by cooling of a hot saturated solution of [**1**]PF_6 in methanol. The analogous reaction of HL_H with $[\{(cod)Ir(\mu\text{-}Cl)\}_2]$ in $MeOH/CH_2Cl_2$, followed by addition of excess KPF_6, led to precipitation of [**2**]PF_6. Crystals of [**2**]PF_6, were obtained by cooling of a saturated solution of [**2**]PF_6 in $MeOH/H_2O$ to 5 °C. The structures of [**1**]PF_6 and [**2**]PF_6 were determined by X-ray diffraction. The X-ray structure of $\mathbf{1}^+$ is shown in Figure 3. $\mathbf{2}^+$ was found to be isostructural. Selected bond lengths and angles for $\mathbf{1}^+$ and $\mathbf{2}^+$ are given in Tables 1 and 2.

Complexes $\mathbf{1}^+$ and $\mathbf{2}^+$ have the expected square-planar geometry. The ligand HL_H is didentate via the pyridine (N_{Py}) and amine (N_{amine}) nitrogens. No interaction is observed between the metal centre and the pyrrole N−H bond (N_{Pyr}−H). In both structures, the N_{Pyr}−H and N^H_{amine} protons are hydrogen bonded to two different PF_6^- counterions ($\mathbf{1}^+$: N_{amine}−F6 distance: 3.165(6) Å, H30−F6 distance: 2.33(7) Å, N_{amine}−H30−F6 angle: 173(6)°, N_{Pyr}−F3 distance: 3.118(6) Å, H20−F3 distance: 2.57(6) Å, N_{Pyr}−H20−F3 angle: 141(6)°; $\mathbf{2}^+$: N_{amine}−F6 distance: 3.098(7) Å, H30−F6 distance: 2.33(7) Å, N_{amine}−H30−F6 angle: 159(6)°, N_{Pyr}−F3 distance: 3.133(7) Å, H20−F3 distance: 2.54(7) Å, N_{Pyr}−H20−F3 angle: 152(8)°). In $[\mathbf{1}]^+$ the Rh−N_{Py} distance [Rh1−N1: 2.101(4) Å] and the Rh−N_{amine} distance [Rh1−N3: 2.144(4) Å] fall within the ranges of Rh−N_{sp2} (2.007−2.140 Å)[5] and Rh−N_{sp3} (2.111−2.178 Å)[5f,6] distances observed for other square planar "N_2"Rh^I(cod) complexes. The observed Rh−C and cod double bond lengths are also normal for "N_2"Rh^I(cod) complexes (Table 1).

The NMR data for [**1**]PF_6 and [**2**]PF_6 in [D_6]acetone are very similar, and are in accordance with their X-ray structure. The largest shift difference between $\mathbf{1}^+$ and $\mathbf{2}^+$ is observed for the *olefinic* cod fragment $(-CH=CH-)_{cod}$ (see Table 3). In the ^{1}H-NMR spectrum of [**1**]PF_6 the pyrrole signals appear at almost the same position as for the free HL_H, whereas the N^H_{amine} proton has shifted 2.75 ppm downfield (HL_H: δ = 2.24, [**1**]PF_6: δ = 4.99). The pyridine-H^6 signal has shifted 0.53 ppm upfield (HL_H: δ = 8.49, [**1**]PF_6: δ = 7.96) as a result of anisotropic shielding by η^4-cod. The N−CH_2−Pyr− and N−CH_2−Py signals appear as singlets at room temp. due to rapid dissociation, pyramidal inversion, and recoordination of N^H_{amine}. Combination of this inversion with rapid rotation of the η^4-cod fragment results in only one signal each for the vinylic, the allylic *exo* and the allyllic *endo* protons of cod. At −80 °C the pyramidal inversion at N_{amine} and rotation of cod are both frozen out. This results in two AB-type doublets for both N−CH_2−Pyr and N−CH_2−Py, each with an additional coupling to the N^H_{amine} proton. At this temperature each cod proton appears as a separate signal, with the exception of two overlapping allylic *exo* protons and two sets of two overlapping allylic *endo* protons.

Complexation of $[Rh^I(cod)]^+$ and $[Ir^I(cod)]^+$ by L_H^-

Reaction of HL_H with $[\{(cod)M^I(\mu\text{-}Cl)\}_2]$ (M = Rh, Ir) in methanol resulted in a solution of $[(HL_H)M^I(cod)]Cl$ M = Rh, Ir). The neutral complexes $[(L_H)M(cod)]$ (M = Rh: **3**; M = Ir: **4**) precipitated upon deprotonation of the uncoordinated pyrrole nitrogen (N_{Pyr}−H) by excess aqueous Na_2CO_3. Cooling of a saturated solution of rhodium

Table 1. Selected bond lengths [Å] for HL_H, **[1]**PF_6, **[2]**PF_6, **3**, $\mathbf{4^A}/\mathbf{4^B}$, **5**, and **6**[a]

	HLH	**[1]**PF_6 (M1 = Rh1)	**[2]**PF_6 (M1 = Ir1)	**3** (M1 = Rh1)	$\mathbf{4^A}$ (M1 = Ir1)	$\mathbf{4^B}$ (M1 = Ir1)	**5** (M1 = Rh)	**6** (M1 = Ir)
N1−M1		2.101(4)	2.083(4)	n. b.	n. b.	n. b	n. b.	2.235(7)
N2−M1		n. b.	n. b.	2.034(3)	2.020(5)	2.023(5)	2.039(3)	2.066(7)
N3−M1		2.144(4)	2.130(4)	2.164(3)	2.147(5)	2.150(5)	2.231(2)	2.397(7)
C12−M1		2.133(4)	2.117(5)	2.117(3)	2.120(6)	2.113(7)	2.106(3)	2.068(8)
C13−M1		2.143(4)	2.127(5)	2.126(3)	2.115(6)	2.098(6)	2.119(3)	2.055(8)
C16−M1		2.154(4)	2.136(5)	2.121(3)	2.125(6)	2.113(7)	2.156(3)	2.136(11)
C17−M1		2.146(4)	2.138(5)	2.145(8)	2.123(6)	2.132(6)	2.146(3)	2.129(10)
C12−C13		1.398(7)	1.403(8)	1.398(5)	1.406(10)	1.429(11)	1.393(5)	1.476(14)
C16−C17		1.392(7)	1.403(8)	1.398(5)	1.411(10)	1.417(10)	1.395(5)	1.414(16)
C6−C7	1.505(7)	1.506(6)	1.492(7)	1.521(5)	1.512(8)	1.519(9)	1.498(4)	1.488(11)
N3−C6	1.454(7)	1.494(6)	1.486(6)	1.458(5)	1.475(8)	1.476(8)	1.507(4)	1.499(11)
C1−C5	1.485(7)	1.479(7)	1.480(8)	1.484(5)	1.484(9)	1.487(9)	1.490(5)	1.493(13)
N3−C5	1.478(7)	1.498(6)	1.520(7)	1.498(4)	1.505(8)	1.506(8)	1.506(5)	1.477(11)
N3−C20	–	–	–	–	–	–	1.497(4)	1.474(12)
Pyridine								
N1−C7	1.331(6)	1.342(6)	1.366(7)	1.334(5)	1.352(9)	1.332(9)	1.356(5)	1.342(11)
C7−C8	1.384(7)	1.386(7)	1.387(7)	1.389(5)	1.377(10)	1.398(10)	1.389(5)	1.407(13)
C8−C9	1.372(8)	1.387(8)	1.386(9)	1.377(5)	1.384(11)	1.361(12)	1.390(7)	1.383(14)
C9−C10	1.369(8)	1.385(8)	1.381(9)	1.361(6)	1.370(12)	1.398(13)	1.373(9)	1.400(15)
C10−C11	1.365(8)	1.375(7)	1.392(8)	1.377(6)	1.385(11)	1.375(12)	1.361(7)	1.366(14)
C11−N1	1.330(7)	1.352(6)	1.336(7)	1.332(5)	1.343(9)	1.346(9)	1.354(5)	1.357(12)
Pyrrole								
N2−C1	1.371(7)	1.361(5)	1.350(8)	1.377(4)	1.384(8)	1.358(8)	1.364(4)	1.354(12)
C1−C2	1.362(7)	1.371(7)	1.371(8)	1.375(5)	1.380(9)	1.387(9)	1.379(4)	1.368(14)
C2−C3	1.408(7)	1.411(8)	1.399(10)	1.419(5)	1.411(10)	1.394(11)	1.403(6)	1.419(16)
C3−C4	1.354(9)	1.350(9)	1.344(11)	1.372(5)	1.382(10)	1.364(10)	1.371(5)	1.361(16)
C4−N2	1.375(6)	1.362(5)	1.360(8)	1.370(4)	1.379(8)	1.380(8)	1.368(4)	1.390(12)

[a] For atom labelling see Figure 2−6. Superscripts A and B refer to crystallographically independent molecules.

complex **3** in toluene resulted in crystals suitable for single-crystal X-ray diffraction. The analogous procedure for iridium complex **4** gave micro-crystalline material with a PXRD-pattern different from that of crystalline **3**. Single crystals of **4**, suitable for X-ray diffraction, could not be obtained from toluene. However X-ray quality crystals of $\mathbf{4} \cdot 1/2\ CH_2Cl_2$ were obtained by cooling a saturated solution in CH_2Cl_2. In the crystal of $\mathbf{4} \cdot 1/2\ CH_2Cl_2$, two independent iridium complexes $\mathbf{4^A}$ and $\mathbf{4^B}$, with geometries slightly different from rhodium complex **3** and from each other, are found in the asymmetric unit. The X-ray structure of **3** is given in Figure 4. Selected bond lengths and angles of **3** and **4** are given in Tables 1 and 2.

Both **3** and **4** have a square planar coordination geometry in which $[L_H]^-$ is didentate via N_{amine} and N_{Pyr}. Thus, deprotonation of $N_{Pyr}-H$ in $[\mathbf{1}]^+$ and $[\mathbf{2}]^+$ to a pyrrolate nitrogen (N_{Pyr}) results in a shift of $[M(cod)]^+$ (M = Rh, Ir) from the $N_{amine}-N_{Py}$ compartment to the $N_{amine}-N_{Pyr}$ compartment (Scheme 2).

In both **3** and $\mathbf{4} \cdot 1/2\ CH_2Cl_2$, N_{Py} accepts an intramolecular hydrogen bond from $N_{amine}-H$ (**3**: $N_{amine}-N_{Py}$ distance: 2.833(4) Å, $H-N_{Py}$ distance: 2.48(4) Å $N_{amine}-H-B_{Py}$ angle 105(3)°; $\mathbf{4^A}$: $N_{amine}-N_{Py}$ distance: 2.815(7) Å, $H-N_{Py}$ distance: 2.43 Å, $N_{amine}-H-N_{Py}$ angle: 104°, $\mathbf{4^B}$: $N_{amine}-N_{Py}$ distance: 2.824(8) Å, $H-N_{Py}$ distance: 2.46 Å, $N_{amine}-H-N_{Py}$ angle: 104°). Whereas in **3** the (*R*) and (*S*) enantiomers occur as monomers, in **4** they dimerise to (*R*,*R*) and (*S*,*S*) via additional intermolecular hydrogen-bonding interactions between $N_{amine}-H$ and N_{Py} (see $\mathbf{4^A}$ and $\mathbf{4^B}$ in Figure 5). [Intermolecular $N_{amine}-N_{Py}$ distances: 3.269(8) Å, 3.216(7) Å; intermolecular $H-N_{Py}$ distances: 2.47 Å, 2.41 Å intermolecular $N_{amine}-H-N_{Py}$ angles: 145°, 145°].

The additional intermolecular hydrogen bonding on going from **3** to **4**, could well reflect that the N^H_{amine} proton of iridium compound **4** is slightly more acidic than the N^H_{amine} proton of rhodium compound **3**, in accordance with its down-field ^{1}H-NMR shift on going from **3** (δ = 4.5) to **4** (δ = 5.3). This might also explain the difference in PXRD-pattern of crystalline **3** and **4** from toluene.

The $M-N_{Pyr}$ distances in **3** and **4** are approx. 0.06 Å shorter than the corresponding $M-N_{Py}$ distances in **[1]**PF_6 and **[2]**PF_6, respectively. This demonstrates the stronger interaction of the anionic pyrrolate nitrogen (N_{Pyr}) with the M^I center. The observed $M-N_{amine}$, $M-C_{olefin}$ and olefinic C−C distances in **3** and **4** are not significantly different from those in **[1]**PF_6 and **[2]**PF_6, respectively. As for $[\mathbf{1}]^+$, the Rh−N, Rh−C and olefinic C−C distances in **3** fall within the normal range for square planar "N_2"Rh^I(cod) complexes.[5][6]

The NMR spectra of **3** and **4** are very similar and correspond well with their solid state structure. As for $[\mathbf{1}]^+$and $[\mathbf{2}]^+$, the largest shift differences between **3** and **4** are observed for $(-CH=CH-)_{cod}$ signals (Table 3). In the ^{1}H-NMR spectrum of rhodium complex **3** at room temp. the pyramidal inversion at N_{amine} is frozen out (AB type signals with additional coupling to the N^H_{amine} proton for $N-CH_2-Py$ and $N-CH_2-Pyr$). Rapid rotation of the η^4-cod fragment results in one signal for the vinylic, two for the allylic *exo* and two for the allylic *endo* protons. The pyridine signals appear at almost the same position as in free HL_H. The N^H_{amine} proton (δ_{NH} = 4.50) has shifted

Table 2. Selected bond angles [°] for HL_H, [**1**]PF_6, [**2**]PF_6, **3**, $\mathbf{4^A/4^B}$, **5**, and **6**[a]

	HLH	[**1**]PF_6 (M1 = Rh1)	[**2**]PF_6 (M1 = Ir1)	**3** (M1 = Rh1)	$\mathbf{4^A}$ (M1 = Ir1)	$\mathbf{4^B}$ (M1 = Ir1)	**5** (M1 = Rh1)	**6** (M1 = Ir1)
N1−M1−N3	−	78.56(15)	78.62(17)	−	−	−	−	69.5(2)
N1−M1−N2	−	−	−	−	−	−	−	94.3(3)
N2−M1−N3	−	−	−	79.89(11)	79.36(19)	79.3(2)	78.15(10)	76.5(3)
N1−M1−C12	−	93.05(17)	92.98(19)	−	−	−	−	168.1(3)
N1−M1−C13	−	99.52(16)	99.62(19)	−	−	−	−	126.3(3)
N1−M1−C16	−	164.81(18)	163.9(2)	−	−	−	−	83.3(4)
N1−M1−C17	−	156.40(18)	156.9(2)	−	−	−	−	99.8(4)
N2−M1−C12	−	−	−	92.68(12)	97.8(2)	93.8(3)	89.89(12)	88.4(4)
N2−M1−C13	−	−	−	97.32(12)	92.6(2)	98.1(2)	96.47(12)	90.9(4)
N2−M1−C16	−	−	−	160.84(13)	159.5(3)	160.4(3)	165.17(13)	165.8(4)
N2−M1−C17	−	−	−	160.73(12)	161.2(2)	159.9(3)	156.92(13)	154.7(4)
N3−M1−C12	−	158.58(18)	157.7(2)	159.44(13)	158.0(2)	160.8(3)	155.54(12)	122.4(3)
N3−M1−C13	−	162.23(18)	162.8(2)	160.95(13)	161.8(2)	158.5(2)	162.83(13)	161.1(3)
N3−M1−C16	−	95.66(17)	95.62(18)	94.72(12)	100.2(2)	94.3(2)	99.33(11)	115.3(3)
N3−M1−C17	−	98.37(17)	98.27(19)	98.88(12)	93.9(2)	98.9(2)	101.11(11)	88.8(3)
C12−M1−C13	−	38.15(19)	38.6(2)	38.49(13)	38.8(3)	39.7(3)	38.50(14)	41.9(4)
C16−M1−C17	−	37.78(19)	38.3(2)	38.00(14)	38.8(3)	39.0(3)	37.82(14)	38.7(4)
M1−N2−C1	−	−	−	115.6(2)	117.0(4)	117.1(4)	114.1(2)	119.1(6)
N2−C1−C5	120.7(4)	−	−	117.3(3)	116.6(5)	116.8(5)	117.4(3)	116.5(8)
C1−C5−N3	111.9(4)	−	−	109.5(3)	108.6(5)	108.6(5)	109.2(3)	111.2(7)
C5−N3−M1	−	−	−	108.0(2)	109.8(4)	108.8(4)	101.81(17)	104.1(5)
M1−N1−C7	−	113.7(3)	113.8(3)	−	−	−	−	119.6(6)
N1−C7−C6	116.1(5)	115.7(4)	115.2(4)	117.6(3)	116.8(6)	117.2(6)	118.2(3)	117.1(8)
C7−C6−N3	112.7(5)	108.8(4)	109.1(4)	114.5(3)	114.7(5)	113.5(5)	114.3(2)	108.1(7)
C6−N3−M1	−	104.1(3)	105.1(3)	−	−	−	−	107.8(5)
Pyrrole								
N2−C4−C3	107.8(5)	107.9(5)	107.8(6)	110.4(3)	109.2(6)	108.9(6)	109.4(3)	110.0(9)
C4−C3−C2	107.8(5)	107.6(5)	107.8(6)	106.9(3)	107.7(6)	108.5(6)	107.4(3)	107.4(10)
C3−C2−C1	107.8(5)	107.5(5)	107.3(6)	105.9(3)	106.2(6)	105.5(6)	106.1(3)	105.0(9)
C2−C1−N2	107.5(5)	107.0(5)	107.1(5)	110.7(3)	110.1(6)	110.4(6)	109.9(3)	112.3(9)
C1−N2−C4	109.1(4)	110.1(5)	109.9(6)	106.0(3)	106.7(5)	106.7(5)	107.1(3)	105.2(8)
Pyridine								
N1−C11−C10	123.7(5)	121.9(5)	122.5(5)	124.5(4)	123.2(7)	123.2(8)	122.9(4)	123.6(9)
C11−C10−C9	118.3(5)	119.8(5)	118.9(5)	118.2(4)	118.3(7)	118.3(8)	119.1(4)	118.9(9)
C10−C9−C8	119.3(5)	118.2(5)	119.1(5)	118.8(4)	119.8(7)	119.1(8)	119.7(5)	118.4(9)
C9−C8−C7	118.7(5)	119.4(5)	119.6(5)	119.2(4)	118.6(7)	118.9(7)	118.7(5)	119.4(7)
C8−C7−N1	122.2(4)	121.9(4)	121.2(5)	122.4(3)	122.7(6)	122.8(6)	121.3(3)	121.8(8)
C7−N1−C11	117.7(4)	118.8(4)	118.8(4)	116.7(3)	117.4(6)	117.6(6)	118.5(4)	117.9(8)

[a] For atom labelling see Figure 2−6. Superscripts A and B refer to crystallographically independent molecules.

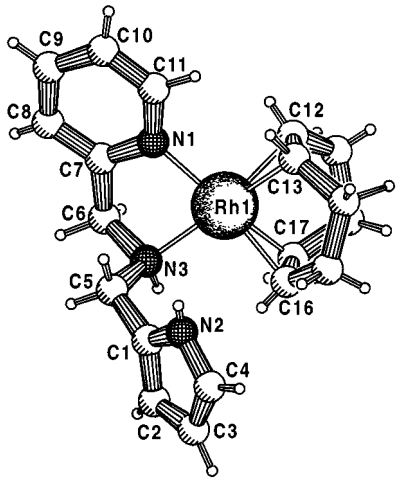

Figure 3. X-ray structure of $[\mathbf{1}]^+$ [only the (*S*) enantiomer is shown]

2.09 ppm downfield from that in the free ligand (δ_{NH} = 2.41). The pyrrole signals have all shifted up-field relative to HL_H. The chemical shift difference is most pronounced for Pyr−H^5 (Pyr−H^5: 0.42 ppm, Pyr−H^4: 0.13 ppm and Pyr−H^3: 0.26 ppm), probably due to anisotropic shielding by the η^4-cod fragment.

Complexation of $[Rh^I(cod)]^+$ and $[Ir^I(cod)]^+$ by $[L_{Bzl}]^-$ and $[L_{Bu}]^-$

Reaction of HL_{Bzl} with $[\{(cod)M^I(\mu\text{-}Cl)\}_2]$ (M = Rh, Ir) in methanol results in a solution of $[(HL_{Bzl})M^I(cod)]Cl$ (M = Rh, Ir). Subsequent addition of an excess of aqueous Na_2CO_3 results in deprotonation of N_{Pyr}−H and precipitation of the neutral complexes $[(L_{Bzl})M^I(cod)]$ (M = Rh: **5**, M = Ir: **6**). $[(L_{Bu})Rh^I(cod)]$, **7**, was obtained analogously. Crystals of **5** and **6** were obtained by cooling of a saturated solution in toluene. Their structures were determined by single-crystal X-ray diffraction (Figure 6). Selected bond lengths and angles are given in Tables 1 and 2.

In the crystal, complex **5** has a square planar geometry with didentate L_{Bzl}^- via N^{Bzl}_{amine} and N_{Pyr}, analogous to L_H^- in **3**. N_{Py} in **5** is not involved in any bonding interaction, whereas N_{Py} in **3** accepts a hydrogen bond from N^H_{amine}. The Rh−N_{Pyr} distances (N2−Rh1) in **5** and **3** are equal within experimental error, but the Rh−N^{Bzl}_{amine} dis-

Table 3. ^1H- and ^{13}C-NMR shifts of $(-HC{=}CH-)_{cod}$

	[1]PF_6[a] (M = Rh)	[2]PF_6[b] (M = Ir)	[3][b] (M = Rh)	[4][b] (M = Ir)	[5][b] (M = Rh)	[6][b] (M = Ir)	[7][c] (M = Rh)
^1H NMR	4.46	4.3 3.38	4.12	3.87 3.73	3.91 3.37	3.47 2.84	3.8 3.40
^{13}C NMR	82.2	68.0 (br)	79.3 78.8	62.3 61.5	77−74 (br)	57−54 (br)	– –

[a] Acetone[D_6]. – [b] CD_2Cl_2. – [c] $CDCl_3$.

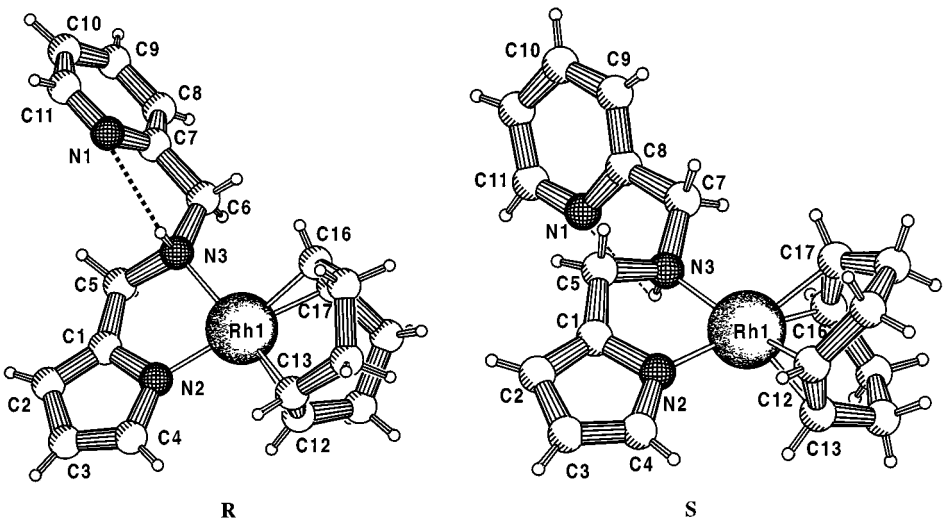

Figure 4. X-ray structure of **3** [the (*R*) and (*S*) enantiomers are shown]

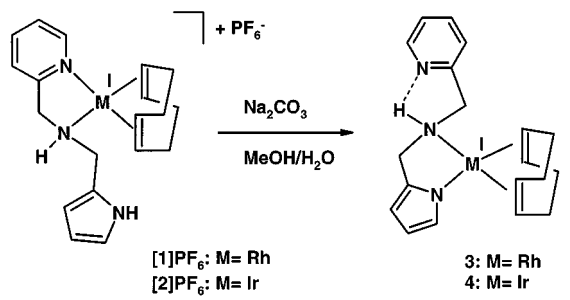

Scheme 2. Dicompartimental ligand HL_H: Shift of $[M^I(cod)]^+$ from $N_{amine}-N_{Py}$ to $N_{amine}-N_{Pyr}$ compartment upon deprotonation of HL_H

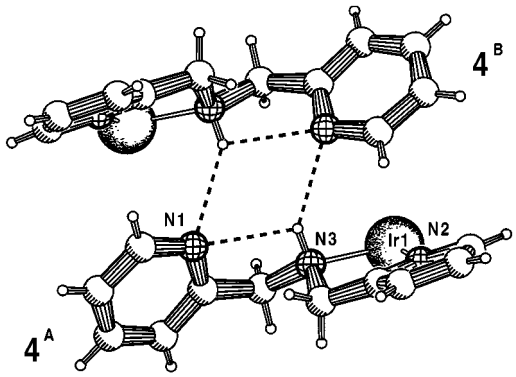

Figure 5. Hydrogen-bonding pattern in the X-ray structure of **4** · 1/2 CH_2Cl_2 [the crystal contains the dimers (*R,R*) and (*S,S*) of the enantiomers (*R*) and (*S*); only *R,R*) is shown]

tance in **5** [N3−Rh1 = 2.231(2) Å] is 0.07 Å longer than the Rh−N^H_{amine} distance in **3** [N3−Rh1 = 2.164(3) Å] and longer than Rh−N_{sp3} distances for square-planar "N_2"-ligand Rh^I complexes (2.111−2.178 Å) known so-far.[5][6] In accordance with this, the Rh−C distances *trans* to N^{Bzl}_{amine} in **5** are approx. 0.04 Å shorter than those trans to N_{Pyr}, whereas the corresponding distances in **3** are not significantly different. These effects all seem to indicate a substantial weakening of the Rh−N^R_{amine} interaction upon substitution of H by Bzl.

In contrast to the four-coordinate rhodium complex **5**, iridium complex **6** is five-coordinate. Complex **6** has a pseudo trigonal-pyramidal geometry with tridentate $[L_{Bzl}]^-$ (Figure 6). N_{Pyr} and one double bond of cod occupy the axial positions, whereas N_{Py} and N_{amine} together with the other double bond of cod occupy the equatorial positions.

Complex **6** contains two chiral centres; N^{Bzl}_{amine} and Ir. Nevertheless only the enantiomeric pairs *S,C* and *R,A*, and not their diastereomers *S,A* and *R,C* are observed. Because of the short "arms" of the ligand, the chiral centre on the amine nitrogen dictates the chirality at the iridium centre during complexation. The *S,A* and *R,C* forms are not accessible due to the geometrical constraints in the ligand.

For d^8-metals in a trigonal-bipyramidal geometry, theoretical and experimental results by Rossi and Hoffmann indicate that the strongest σ-donor prefers the axial position and that olefins are more strongly bound in the equatorial plane.[7] The axial position of the strongest σ-donor,

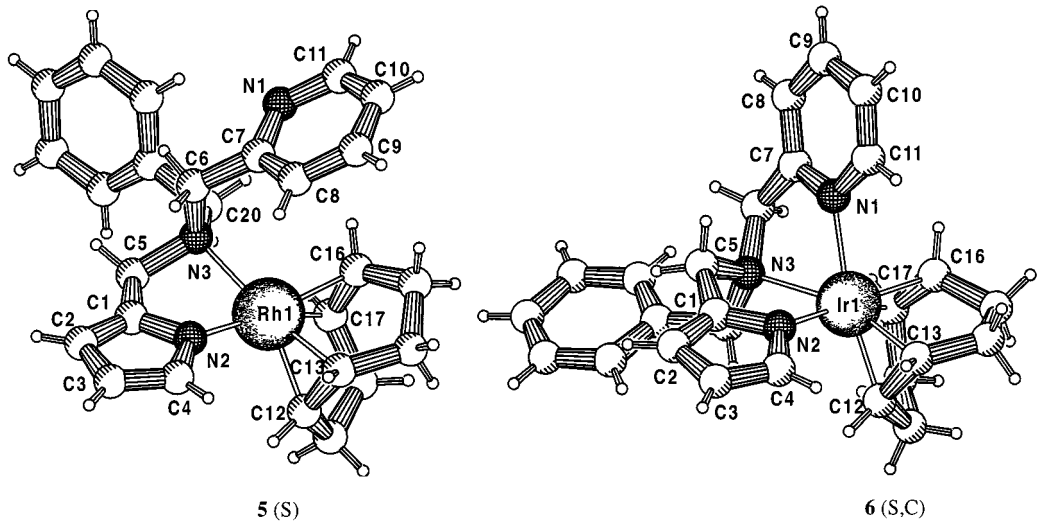

Figure 6. X-ray structures of **5** (*S* enantiomer) and **6** (*S,C* enantiomer), corresponding with enantiomer (*S*) of **3** in Figure 4

N_{Pyr}, at the shortest Ir−N distance (Ir−N2: 2.066 Å) and the shorter Ir−C distances for the equatorial double bond [Ir1−C12: 2.068(8) Å, Ir1−C13: 2.055(8) Å] relative to the axial double bond [Ir1−C16: 2.136(11) Å, Ir1−C17: 2.129(10) Å] are in accordance with theoretical and experimental results by Rossi and Hoffmann. In accordance with its "unfavourable" equatorial position, the $M-N^{Bzl}_{amine}$ distance (M1−N3) in the five-coordinate iridium complex **6** exceeds the $M-N^{Bzl}_{amine}$ distance in four-coordinate rhodium complex **5** by 0.17 Å, whereas the $M-N_{Pyr}$ distance (M−N2) in the "favourable" axial position is not significantly longer than in **5** (Table 1). Interestingly, **5** undergoes $\kappa^2-\kappa^3$ isomerisation on going from the solid state to solution (Scheme 3).

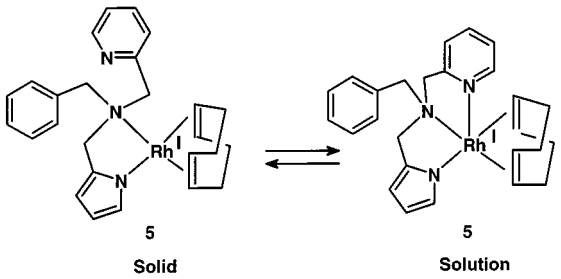

Scheme 3. $\kappa^2-\kappa^3$ isomerism for L_{Bzl}^- in **5**

In the ^{1}H-NMR solution spectrum of **5**, Py-H^6 of L_{Bzl}^- has shifted 0.69 ppm downfield relative to Py-H^6 of free HL_{Bzl} (HL_{Bzl}: δ = 8.56, HL_{Bzl}^- in **5**: δ = 9.25). This is in marked contrast with the situation for **3**, where we observed no significant shifts for Py-H^6 of the uncoordinated pyridine group of L_H^- compared to free HL_H (HL_H: δ = 8.48, L_H^- in **3**: δ = 8.55). Also, the Py-H^6 signal in **5** shows clear NOE contacts (counter phase to diagonal) with Pyr-H^5, and the two vinylic and the two allylic *exo* signals of cod. This shows that the structure of **5** in solution is predominantly five-coordinate. As was the case for $[\mathbf{1}]^+$ and **3**, the ^{1}H-NMR spectrum of **5** shows rapid rotation of the η^4-cod fragment. Two signals are observed for the vinylic protons, one for the allylic *exo* protons, and one for the allylic *endo* protons. At room temperature pyramidal inversion at N^{Bzl}_{amine} is slow on the ^{1}H-NMR time-scale (two AB-type doublets for each, $N-CH_2-Py$, $N-CH_2-Pyr$, and $N-CH_2-Ph$), but fast on the NOESY/EXSY time scale (exchange correlation peaks were observed for the two vinylic proton signals and for H_a and H_b of the three AB-patterns). On the basis of its ^{1}H-NMR spectrum, the solution structure of butylamine derivative **7** is similar to that of benzylamine derivative **5** (Table 3). As for **5**, the significant downfield shift of Py-H^6 (Δδ = 0.58 ppm) indicates that L_{Bu}^- is tridentate in solution.

Complex **6**, the iridium analogue of **5**, is also five-coordinate in solution. However **6** does not show N^{Bzl}_{amine} inversion on the ^{1}H-NOESY/EXSY time-scale. This seems to indicate the stronger preference of iridium for five-coordination.[8] Apart from the chemical shift differences for $(-HC=CH-)_{cod}$ (Table 3), the NMR spectra of **5** and **6** are very similar.

Thus, substitution of the N^H_{amine} proton in **3/4** by benzyl in **5/6** or butyl in **7** induces N_{Py} coordination in solution. This appears to be triggered by a weaker $N_{amine}-Rh$ interaction resulting from steric repulsions, and by the loss of stabilisation of the uncoordinated N_{Py} through hydrogen bonding with $N_{amine}-H$.

The ^{13}C-NMR signals for $(-CH=CH-)_{cod}$ of the iridium complexes appear at significant lower values than their corresponding rhodium analogues (Table 3), indicating stronger π-back donation for iridium.[8] Both for rhodium and for iridium, significant upfield shifts are observed for the $(-CH=CH-)_{cod}$ NMR signals on going from four-coordination to five-coordination (Table 3). The average NMR signals of $(-CH=CH-)_{cod}$ of four-coordinate **3** and **4** in CD_2Cl_2 [**3**: δ(^{1}H) = 4.1 and δ(^{13}C) = 79; **4**: δ(^{1}H) = 3.8 and δ(^{13}C) = 62] appear at significantly higher values than those of five-coordinate **5** and **6** [**5**: δ(^{1}H) = 3.6 and δ(^{13}C) = 77−74 (br); **6**: δ(^{1}H) = 3.2 and δ(^{13}C) = 57−54(br)]. For **7**, δ(^{1}H) = 3.7, which is close to the value

of **5**. This situation parallels that for 3,5-disubstituted tris(pyrazolyl)borate (Tp^{R2}) rhodium(I) cod complexes, where in $CDCl_3$ $\delta(^1H) = 4.1$ and $\delta(^{13}C) = 80$ for four-coordinate $[(\kappa^2\text{-}Tp^{R2})Rh^I(cod)]$ and $\delta(^1H) = 4.0$ and $\delta(^{13}C) = 73$ for five-coordinate $[(\kappa^3\text{-}Tp^{H2})Rh^I(cod)]$.[12e]

Reactivity towards H_2O, O_2, and H_2O_2

Solutions of the pyridine-amine-pyrrolate complexes **3**, **4**, **5**, **6**, and **7** show no reactivity towards water, but are oxidised in a nonselective way by air and aqueous H_2O_2. Sparingly soluble precipitates result, which have complex ^1H-NMR spectra with very broad lines.

Catalytic Polymerisation of Phenylacetylene

Complexes **5** and **7** are neutral "N_3"$Rh^I(cod)$ complexes that show $\kappa^2-\kappa^3$ isomerism, similar to tris(pyrazolyl)borate rhodium(I) cod complexes. Isomerisation of $[(\kappa^3\text{-}Tp^{R2})Rh^I(cod)]$ to $[(\kappa^2\text{-}Tp^{R2})Rh^I(cod)]$ has been suggested to be essential for its catalytic activity in the polymerisation of phenylacetylene.[9] In accordance with this we observed that rhodium complex **5**, but not iridium complex **6,** is an active catalyst for the polymerisation of phenylacetylene (Scheme 4).

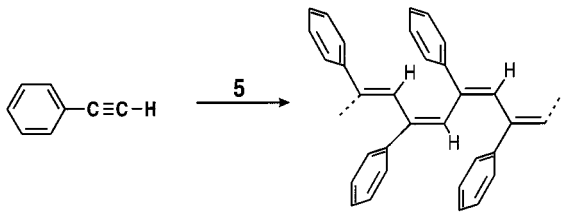

Scheme 4. Polymerisation of phenylacetylene by **5**

Reaction of phenylacetylene in MeOH in the presence of 0.1 mol-percent of **5** resulted in precipitation of yellow poly(phenylacetylene) in 24% yield within 20 min. The molecular mass (M_n) and the high stereoregularity (head-to-tail cis-transoidal structure) of the obtained poly(phenylacetylene) are similar to those of poly(phenylacetylene) prepared with $(Tp^{R2})Rh^I(cod)$[9] and other rhodium catalysts.[10] The broad molecular weight distribution ($M_w/M_n = 4.7$) could be the result of partial precipitation during polymerisation.

Discussion

The pyridine-amine-pyrrolate complexes **3**−**7** are not oxidised selectively by H_2O_2 or O_2. Oxidation of the negatively charged pyrrolate group is probably responsible for these aselective oxidations. The new pyridine-amine-pyrrole and pyridine-amine-pyrrolate ligands display a diverse coordination chemistry towards $[Rh^I(cod)]^+$ and $[Ir^I(cod)]^+$.

The neutral pyridine-amine-pyrrole ligand HL_H in $[\mathbf{1}]^+$ and $[\mathbf{2}]^+$ is didentate via N^H_{amine} and N_{Py}. Deprotonation of the pyrrole group results in the potentially tridentate pyridine-amine-pyrrolate ligands L_H^-, L_{Bzl}^- and L_{Bu}^-. In both **3** (M = Rh) and **4** (M = Ir), L_H^- is didentate via N^H_{amine} and N_{Pyr} in the solid state *and* in solution. The observed difference between **3** and **4** in the solid state could well reflect that the N^H_{amine} proton of iridium compound **4** is slightly more acidic than the N^H_{amine} proton of rhodium compound **3**, in accordance with the down-field shift of the N^H_{amine} proton in the ^1H-NMR spectrum on going from **3** to **4**. The higher acidity is probably the result of stronger metal−ligand interaction for iridium(I) than for rhodium(I). In accordance with this, the ^{13}C-NMR olefinic cod signals of the iridium complexes are observed at higher field than those of their rhodium analogues (see Table 3).

L_{Bzl}^- in **5** (M = Rh) is predominantly tridentate via N_{Pyr}, N_{amine}, and N_{Py} in solution, but didentate via N_{Pyr} and N_{amine} in the solid state. Apparently, the free energy increase on going from κ^3-L_{Bzl} to κ^2-L_{Bzl} can easily be overcome by packing forces. The ^1H-NMR spectrum of **5** shows the occurrence of another mode of $\kappa^2-\kappa^3$ isomerism in solution, involving dissociation, pyramidal inversion and recoordination of N^{Bzl}_{amine}. The activity of **5** in polymerisation of phenylacetylene also reflects the occurrence of $\kappa^2-\kappa^3$ isomerism. L_{Bzl}^- in **6**, the Ir-analogue of **5**, shows no sign of pyramidal inversion of N^{Bzl}_{amine} via $\kappa^2-\kappa^3$ isomerism in solution, and is tridentate in the solid state. The observed differences between **5** and **6** in solution and in the solid state both appear to reflect the higher tendency of iridium for five coordination.[8]

Previously, $\kappa^2-\kappa^3$-isomerism has been observed for 3,5-disubstituted tris(pyrazolyl)borate[11] (Tp^{R2}) complexes $[(Tp^{R2})Rh^I(L_2)]$ (L_2 = diolefin or $(olefin)_2$).[12][13] Whereas a bulky R at the pyrazolyl-3-position in $[(Tp^{R2})Rh^I(cod)]$ favours four-coordination over five-coordination ($\kappa^2 > \kappa^3$), a bulky R at N^R_{amine} in $[(L_R^-)Rh^I(cod)]$ favours five-coordination over four-coordination ($\kappa^3 > \kappa^2$). Increased steric repulsion at N^R_{amine} in $[(L_R^-)Rh^I(cod)]$ induces a weaker $Rh-N^R_{amine}$ interaction. This is compensated by additional coordination of N_{Py}, and thus results in five coordination.

Experimental Section

General Methods: All reactions were performed under a nitrogen atmosphere using standard schlenk techniques, unless mentioned otherwise. Solvents (p. a.) were deoxygenated by bubbling through a stream of N_2 or by the freeze-pump-thaw method. The temperature indication room temp. corresponds to ca. 20 °C. $[\{(cod)Rh(\mu\text{-}Cl)\}_2]$[14] and $[\{(cod)Ir(\mu\text{-}Cl)\}_2]$[15] were prepared according to a literature procedure. All other chemicals are commercially available and were used without further purification. − IR spectra were measured on a Perkin−Elmer 1720X. − NMR experiments were carried out on a Bruker DPX200 (200 MHz and 50 MHz for ^1H and ^{13}C respectively), a Bruker AC300 (300 MHz and 75 MHz for ^1H and ^{13}C respectively) and a Bruker AM500 (500 MHz and 125 MHz for ^1H and ^{13}C respectively). Solvent shift reference for ^1H NMR: $[D_6]$acetone $\delta_H = 2.05$, THF-$[D_8]$ $\delta_H = 1.72$, CD_2Cl_2 $\delta_H = 5.31$, $CDCl_3$ $\delta_H = 7.28$. For ^{13}C NMR: $[D_6]$acetone $\delta_C = 29.50$, CD_2Cl_2 $\delta_C = 54.20$. Abbreviations used are s = singlet, d = doublet, dd = doublet of doublets, ddd = doublet of doublets of

doublets, t = triplet, m = multiplet and br = broad. − Elemental analysis (C,H,N) were carried out on a Carlo Erba NCSO-analyser. − Mass Spectra were recorded on a VG 7070 Mass spectrometer (FAB/EI) or on a JEOL JMS SX/SX102A four sector mass spectrometer (FD).

X-ray Diffraction: Crystals of [**1**]PF_6 and [**2**]PF_6 suitable for X-ray diffraction studies were obtained by cooling a saturated solution of the corresponding compound in MeOH to −20 °C. Crystals of HL_H, **3**, **5**, and **6** suitable for X-ray diffraction studies were obtained from hot saturated toluene solutions. Crystals of **4** suitable for X-ray diffraction studies were obtained by slow crystallisation from a saturated CH_2Cl_2 solution at −20°C. Single crystals were mounted in air on glass fibres. For [**1**]PF_6, [**2**]PF_6, **4**, **5**, and **6** an Enraf−Nonius CAD4 single-crystal diffractometer was used, graphite monochromatised Cu-*Kα* radiation, θ-2θ scan mode. The X-ray diffraction data for **3** were collected on a Enraf−Nonius CAD4T rotating anode diffractometer, graphite monochromatised Mo-*Kα* radiation, ω-scan mode. Semi-empirical absorption correction (*ψ*-scan) was applied.[16]

For HL_H an Enraf−Nonius CAD4 single-crystal diffractometer was used, graphite monochromatised Mo-*Kα* radiation, θ-2θ scan mode. No absorption correction was applied. Structures [**1**]PF_6, [**2**]PF_6, **3**, **4**, **5**, and **6** were solved by the program system DIRDIF[17] using the program PATTY[18] to locate the heavy atoms. The structure of HL_H was solved using the program CRUNCH.[19] All structures were refined with standard methods (refinement against F^2 of all reflections with SHELXL97[20]) with anisotropic parameters for the nonhydrogen atoms. Intensity data were corrected for Lorentz and polarisation effects. All hydrogen atoms were placed at calculated positions and were subsequently freely refined, however, for **4** and **6**, the hydrogen atoms were placed at calculated positions and were refined riding on the parent atoms. Details of the crystal parameters, data collections and structure refinements are given in Table 4. Crystallographic data (tables of structure determinations summaries, lists of anisotropic displacement parameters, lists of atom coordinates and full lists of bond lengths and angles, excluding structure factors) have been deposited with the Cambridge Crystallographic Data Centre as supplementary publication no. CCDC-115640 ([**1**]PF_6), 115641 (**3**), 115642 (**5**), 115643 (HL_H), 115644 ([**2**]PF_6), 115645 (**6**), and 115646 (**4**). Copies of the data can be obtained free of charge on application to The Director, CCDC, 12 Union Road, Cambridge CB2 1EZ, UK (fax: Int. Code +44 (1223) 336-033; E-mail: deposit@chemcrys.cam.ac.uk)

Syntheses

***N*-(2-Pyridylmethyl)-*N*-(1*H*-2-pyrrolylmethyl)amine (HL_H):** 6.8 g (0.064 mol) of 1*H*-pyrrole-2-carboxaldehyde was dissolved in 60 mL of EtOH and 6.0 g (0.063 mol) of picolylamine was added dropwise. The solution was heated to reflux for 10 min. Evaporation of the solvent under vacuum results in a yellow powder, from which *N*-(2-pyridylmethyl-*N*-(1*H*-pyrrolylmethylidene)amine was obtained as a white solid by recrystallisation from a hot saturated Et_2O solution. Yield 11.5 g (0.062 mol, 98%). − 11.3 g (0.061 mol) of *N*-(2-pyridylmethyl-*N*-(1*H*-pyrrolylmethylidene)amine was then dissolved in 200 mL of deoxygenated methanol. The solution was cooled to −10°C, and 2.9 g (0.076 mol) of $NaBH_4$ was added and some gas evolved from the solution. The solution was heated to 50°C for 3 h after which the solvent was partially evaporated. To this solution 50 mL water was added to destroy the excess $NaBH_4$. The water layer was extracted three times with 30 mL of Et_2O, and the combined Et_2O-fractions were dried with 10 g of $MgSO_4$. Filtration and evaporation of the solvent results in *N*-(2-pyridylmethyl)−*N*-(1*H*-2-pyrrolylmethyl)amine (HL_H) as a yellow powder, and was recrystallised from a hot saturated Et_2O solution. Yield 10.3 g (0.055 mol, 90%). Colourless crystals suitable for X-ray diffraction were obtained by crystallisation from toluene. − Mp: 59.0°C. − ^{1}H NMR (200 MHz, CD_2Cl_2, 298 K): δ = 9.40 (s, b, 1 H, Pyr−H1), 8.54 [d,1 H, ^3J(H,H) = 4.1 Hz, Py−H6], 7.65 [t, 1 H, ^3J(H,H) = 7.6 Hz, Py−H4], 7.26 [d, 1 H, ^3J(H,H) = 7.6 Hz, Py−H3], 7.16 [dd, 1 H, ^3J(H,H) = 7.6 Hz, ^3J(H,H) = 4.1 Hz, Py−H5], 6.67 (m, Pyr−H5), 6.05 (m, 1 H, Pyr−H4), 5.98 (m, 1 H, Pyr−H3), 3.86 (s, 2 H, N−CH_2−Py), 3.78 (s, 2 H, N−CH_2−Pyr), 2.41 (s, br, 1 H, NH). − ^{13}C {^{1}H} (75 MHz, [D$_6$]acetone, 298 K): δ = 161.4 (Py−C2), 149.9 (Py−C6), 137.2 (Py−C4), 131.6 (Pyr−C2), 122.9 (Pyr−C5), 122.2 (Py−C5), 117.8 (Py−C3), 108.7 (Pyr−C4), 106.9 (Pyr−C3), 54.9 (N−CH_2−Pyr), 46.8 (N−CH_2−Py). − EI-MS (*m*/*z*): 185 $[M]^+$, 118 $[M - Pyr + H]^+$, 107 $[M - CH_2Py]^+$, 93 $[CH_2Py + H]^+$. − $C_{11}H_{13}N_3$ (187.24): calcd. C 70.56, H 7.00, N 22.44; found C 70.55, H 7.03, N 21.95.

***N*-Benzyl-*N*-(2-pyridylmethyl)-*N*-(1*H*-2-pyrrolylmethyl)amine (HL_{Bzl}):** 9.5 g (0.09 mol) of 1*H*-pyrrole-2-carboxaldehyde was dissolved in 50 mL of freshly distilled THF and cooled to 0°C. 10.7 g (0.10 mol) of benzylamine was added drop wise. After 15 min the solution was allowed to warm up to room temp. and was stirred for 10 h. Evaporation of the solvent under vacuum results in a yellow powder, from which *N*-benzyl-*N*-(1*H*-pyrrolylmethylidene)-amine was obtained as a white solid by recrystallisation from a hot saturated Et_2O solution. Yield 17.7 g (0.085 mol, 96%). 9.2 g (0.049 mol) of *N*-benzyl-*N*-(1*H*-pyrrolylmethylidene)amine was then dissolved in 60 mL of deoxygenated methanol. The solution was cooled to 0°C, and 2.0 g (0.053 mol) of $NaBH_4$ was added and some gas evolved from the solution. The solution was heated to 50°C for 10 h after which the solvent was partially evaporated. To this solution 50 mL of water was added to destroy the excess $NaBH_4$. The water layer was extracted three times with 30 mL of Et_2O, and the combined Et_2O fractions were dried with 10 g of $MgSO_4$. Filtration and evaporation of the solvent results in 1*H*-pyrrol-2-ylmethylbenzylamine as a yellow oil, sufficiently pure for further reaction. Yield 7.87 g (0.061 mol, 71.3%). 100 mL of methanol was cooled to 0°C and 12 g of Na_2CO_3, dissolved in 20 mL of water, was added. To the resulting suspension 6.89 g (0.042 mol) of picolyl chloride hydrochloride and 7.9 g (0.042 mol) of (1*H*-pyrrol-2-ylmethyl)benzylamine were added. The pink solution was stirred for 10 h and gradually changed its colour to orange. The mixture was filtered and the filtrate was evaporated yielding a crude red solid. *N*-benzyl-*N*-(2-pyridylmethyl)-*N*-(1*H*-2-pyrrolylmethyl)amine (HL_{Bzl}) was obtained as a white solid by recrystallisation from a saturated Et_2O solution at −20°C. Yield 4.46 g (0.016 mol, 38%). − Mp: 86.0°C. − ^{1}H NMR (200 MHz, CD_2Cl_2, 298 K): δ = 9.84 (s, br, 1 H, Pyr−H1), 8.56 (m,1 H, Py−H6), 7.70 (m, 1 H, Py−H4, Py−H3), 7.8−7.2 (m, 6 H, Ph−H, Py−H4, Py−H5), 6.79 (m, Pyr−H5), 6.08 (m, 1 H, Pyr−H4), 5.99 (m, 1 H, Pyr−H3), 3.65 (s, 2 H, N−CH_2−Py), 3.62 (s, 2 H, N−CH_2−Pyr), 3.52 (s, 2 H, N−CH_2−Ph). − ^{13}C {^{1}H} (75 MHz, [D$_6$]acetone, 298 K): δ = 161.1 (Py−C2), 149.9 (Py−C6), 141.0 (Pyr−C2), 137.6 (Py−C4), 130.0 (Ph−C2, Ph−C3), 129.4 (Ph−C4), 128.1 (Ph−C1), 124.3 (Pyr−C5), 123.2 (Py−C5), 118.5 (Py−C3), 108.8 (Pyr−C4), 108.6 (Pyr−C3), 59.9 (N−CH_2−Ph), 58.9 (N−CH_2−Pyr), 51.1 (N−CH_2−Py). − EI-MS [*m*/*z* (%)]: 277 $[M]^+$ (0.13), 211 $[M - Pyr]^+$ (0.10), 197 $[M - CH_2Pyr]^+$ (37.10), 185 $[M - CH_2Py]^+$ (75.34), 93 $[CH_2Py + H]^+$ (100). − $C_{18}H_{19}N_3$ (277.37): calcd. C 77.95, H 6.90, N 15.15; found C 77.81, H 6.90, N 14.75.

***N*-Butyl-*N*-(2-pyridylmethyl)-*N*-(1*H*-2-pyrrolylmethyl)amine (HL_{Bu}):** *N*-Butyl-*N*-(2-pyridylmethyl)-*N*-(1*H*-2-pyrrolylmethyl)am-

Table 4. Crystallographic data for HL_H, [**1**]PF_6, [**2**]PF_6, **3**, **4** · 1/2 CH_2Cl_2, **5**, and **6**

	HL_H	[**1**]PF_6	[**2**]PF_6	**3**	**4** · 1/2 CH_2Cl_2	**5**	**6**
Emperical formula	$C_{11}H_{13}N_3$	$C_{19}H_{25}F_6N_3PRh$	$C_{19}H_{25}F_6IrN_3P$	$C_{19}H_{24}N_3Rh$	$C_{19.5}H_{25}ClIrN_3$	$C_{26}H_{30}N_3Rh$	$C_{26}H_{30}IrN_3$
Crystal size [mm]	0.37×0.33×0.29	0.37×0.33×0.17	0.25×0.22×0.12	0.22×0.22×0.12	0.48×0.16×0.06	0.46×0.29×0.20	0.17×0.13×0.12
Formula mass	187.24	543.30	632.59	397.32	529.08	487.44	576.73
T [K]	293(2)	208(2)	208(2)	173(2)	208(2)	293(2)	208(2)
Crystal system	Monoclinic	Triclinic	Triclinic	Monoclinic	Triclinic	Triclinic	Monoclinic
Space group	$C2/c$	$P-1$	$P-1$	$P2_1/c$	$P-1$	$P-1$	$P\,2_1/n$
a [Å]	15.85(4)	9.63157(17)	9.6377(3)	11.2479(5)	10.3279(3)	10.2385(3)	9.2972(6)
b [Å]	10.8942(15)	9.7229(3)	9.7205(3)	14.8328(8)	13.0692(3)	10.2554(2)	16.1521(8)
c [Å]	12.22(3)	13.8150(3)	13.7985(9)	10.3258(6)	15.1735(3)	11.2513(4)	14.8152(9)
α [°]	90	75.425(3)	75.408(6)	90	96.837(3)	79.957(3)	90
β [°]	106.5(3)	69.0584(17)	68.963(3)	111.157(4)	103.634(3)	72.835(3)	102.105(5)
γ [°]	90	60.680(3)	60.599(5)	90	105.233(2)	77.666(2)	90
V [Å^3]	2025(6)	1048.82(4)	1046.57(8)	1606.62(15)	1884.32(8)	1094.83(6)	2175.3(2)
$\rho_{calcd.}$ [gcm^{-3}]	1.229	1.720	2.007	1.643	1.865	1.479	1.761
Z	8	2	2	4	4	2	4
Diffractometer (scan)	Enraf−Nonius CAD4 (θ−2θ)	Enraf−Nonius CAD4 (θ−2θ)	Enraf−Nonius CAD4 (θ−2θ)	Nonius CAD4T rotating anode (ω−scan)	Enraf−Nonius CAD4 (θ−2θ)	Enraf−Nonius CAD4 (θ−2θ)	Enraf−Nonius CAD4 (θ−2θ)
Radiation	Mo-K_α	Cu-K_α	Cu-K_α	Mo-K_α	Cu-K_α	Cu-K_α	Cu-K_α
Wavelength [Å]	0.71073	1.54184	1.54184	0.71073	1.54184	1.54184	1.54184
F(000)	800	548	612	816	1028	504	1136
θ range [°]	2.64 to 26.26	3.44 to 69.97	3.44 to 69.97	1.94 to 27.46	3.05 to 69.90	4.14 to 69.95	4.10 to 70.02
Index ranges	$0 \le h \le 19$	$-11 \le h \le 10$	$-11 \le h \le 10$	$-14 \le h \le 14$	$-12 \le h \le 12$	$-12 \le h \le 12$	$-11 \le h \le 11$
	$0 \le k \le 13$	$-11 \le k \le 0$	$-11 \le k \le 11$	$-7 \le k \le 19$	$0 \le k \le 15$	$0 \le k \le 12$	$-19 \le k \le 19$
	$-15 \le l \le 14$	$-16 \le l \le 16$	$-16 \le l \le 0$	$-13 \le l \le 13$	$-18 \le l \le 18$	$-13 \le l \le 13$	$-18 \le l \le 0$
Range of rel. transm. fac.	−	0.784/1.655	0.827/1.515	0.964/1.049	0.724/2.183	0.790/1.373	0.816/1.227
Measured reflections	2095	4231	4145	7391	7465	4410	8395
Unique reflections	2022	3977	3970	3674	7130	4159	4120
Observed refl. [$Io > 2\sigma(Io)$]	1252	3936	3964	2799	6975	4145	3476
Refined parameters	180	372	372	304	443	392	271
Goodness-of-fit on F^2	1.166	1.135	1.144	1.023	1.117	1.123	1.051
R [$Io > 2\sigma(Io)$]	0.0915	0.0403	0.0309	0.0358	0.0427	0.0335	0.0674
$wR2$[all data]	0.3156	0.1331	0.0847	0.0732	0.1255	0.0934	0.1920
ρ_{fin} (max/min) [eÅ^{-3}]	0.352/−0.314	1.764/−1.463	2.103/−2.243	0.797/−0.395	3.732/−2.130	1.627/−1.125	6.529/−5.715

ine (HL_{Bu}) was obtained as a red oil by a procedure similar to that of *N*-benzyl-*N*-(2-pyridylmethyl)-*N*-(1*H*-2-pyrrolylmethyl)amine (HL_{Bzl}), starting from *n*-butylamine instead of benzylamine. The compound was purified by column chromatography over silica-60H with 10% MeOH/$CHCl_3$. Yield 0.64 g (2.63 mmol, 15.5%). − ^{1}H NMR (200 MHz, $CDCl_3$, 298 K): δ = 9.83 (s, br, 1 H, Pyr−H1), 8.52 [d, 1 H, ^3J(H,H) = 3.2 Hz, Py−H6], 7.61 (m, 1 H, Py−H4), 7.45 (m, 1 H, Py−H3), 7.15 (m, 1 H, Py−H5), 6.78 (m, 1 H, Pyr−H5), 6.11 (m, 1 H, Pyr−H4), 6.01 (m, 1 H, Pyr−H3), 3.69 (s, 2 H, N−CH_2−), 3.59 (s, 2 H, N−CH_2−), 2.48 [t, 2 H, ^3J(H,H) = 7.4 Hz, N−CH_2−C_3H_7], 1.51 (m, 2 H, N−CH_2−CH_2−C_2H_5), 1.31 (m, 2 H, N−C_2H_4−CH_2−CH_3), 0.85 [t, 3 H, ^3J(H,H) = 7.1 Hz, N−C_3H_6−CH_3]. − EI-MS [*m*/*z* (%)]: 244 $[M]^+$ (3), 186 $[M - Bu]^+$ (4), 163 $[M - Py]^+$ (39), 151 $[M - Bu - Pyr]^+$ (84), 107 $[M - Bu - Py]^+$, 93 $[CH_2Py + H]^+$ (100).

(η^4-Cycloocta-1,5-diene)[*N*-(2-pyridylmethyl)-*N*-(1*H*-2-pyrrolylmethyl)amine]rhodium(I) Hexafluorophosphate ([1]PF_6): 30.0 mg (0.16 mmol) of *N*-(2-pyridylmethyl)-*N*-(1*H*-2-pyrrolylmethyl)amine (HL_H) was dissolved in 5 mL of MeOH and 39.5 mg (0.08 mmol) of $[\{(cod)Rh(\mu\text{-}Cl)\}_2]$ was added, and stirred at room temp. for 1 h. Addition of 32.6 mg of NH_4PF_6 resulted in the precipitation of $[(HL_H)Rh^{I}(cod)]PF_6$ ([**1**]PF_6) as a yellow solid, which was collected by filtration, washed with small portions of water and MeOH and was vacuum-dried. Crystals suitable for X-ray diffraction were obtained by slow crystallisation from a saturated MeOH solution at −20°C. Yield 54 mg (62%). − ^{1}H NMR (500 MHz, [D$_6$]acetone, 298 K): 10.22 (s, br, 1 H, Pyr−H1), 8.10 [ddd, 1 H, ^3J(H,H) = 7.83 Hz, ^3J(H,H) = 7.10 Hz, ^4J(H,H) = 1.46 Hz, Py−H4], 7.96 [d, 1 H, ^3J(H,H) = 5.88 Hz, Py−H6], 7.76 [d, 1 H, ^3J(H,H) = 7.83 Hz, Py−H3], 7.54 [dd, 1 H, ^3J(H,H) = 7.10 Hz, ^3J(H,H) = 5.88 Hz, Py−H5], 6.80 (m, 1 H, Pyr−H5), 6.29 (m, 1 H, Pyr−H3), 6.06 (m, 1 H, Pyr−H4), 4.99 (s, br, 1 H, NH), 4.46 (m, br, 4 H, −HC=CH−), 3.98 (s, 2 H, N−CH_2−), 3.95 (s, 2 H, N−CH_2−), 2.47 (m, br, 4 H, −C=C−$CH_{2\ exo}$), 1.98 (m, br, 4 H, −C=C−$CH_{2\ endo}$). − ^{1}H NMR (500 MHz, [D$_6$]acetone, 193 K): δ = 10.65 (s, br, 1 H, Pyr−H1), 8.12 [ddd, ^3J(H,H) = 7.4 Hz, ^3J(H,H) = 7.4 Hz, ^4J(H,H) = 1.5 Hz, Py−H4], 7.98 [d, 1 H, ^3J(H,H) = 5.5 Hz, Py−H6], 7.79 [d, 1 H, ^3J(H,H) = 7.4 Hz, Py−H3], 7.56 [dd, 1 H, ^3J(H,H) = 7.4 Hz, ^3J(H,H) = 5.5 Hz, Py−H5], 6.87 [d, 1 H, ^3J(H,H) = 1.5 Hz, Pyr−H5], 6.25 (m, 1 H, Pyr−H3), 6.06 (m, 1 H, Pyr−H4), 5.16 (s, br, 1 H, NH), 4.74 (s, br, 1 H, −*HC*=*CH*−), 4.57 {dd[AB], 1 H, ^2J(H,H) = 16.0 Hz, ^3J(H,H) = 4.8 Hz, N−CH_2−}, 4.51 (s, br, 1 H, −*HC*=*CH*−), 4.30 {dd[AB], 1 H, ^2J(H,H) = 16.0 Hz, ^3J(H,H) = 2.9 Hz, N−CH_2−}, 3.95 {dd[AB], 1 H, ^2J(H,H) = 14.0 Hz, ^3J(H,NH) = 6.6 Hz, N−CH_2−}, 3.86 {dd[AB], 1 H, ^2J(H,H) = 14.0 Hz, ^3J(H,NH) = 6.6 Hz, N−CH_2−}, 3.64 (s, br, 1 H, −*HC*=*CH*−), 2.58 (m, br, 1 H, −C=C−$CH_{2\ exo}$), 2.46 (m, br, 1 H, −C=C−$CH_{2\ exo}$), 2.30 (m, br, 2 H, −C=C−$CH_{2\ exo}$), 2.02 (m, br, 2 H, −C=C−$CH_{2\ endo}$), 1.85 (m, br, 2 H, −C=C−$CH_{2\ endo}$). − ^{13}C NMR (50 MHz, [D$_6$]-acetone, 298 K): δ = 161.5 (Py−C2), 147.8 (Py−C6), 139. 8 (Py−C4), 124.8 (Pyr−C2), 124.0 (Py−C3), 122.9 (Py−C5), 118.6 (Pyr−C5), 109.6 (Pyr−C4), 108.2 (Pyr−C2), 82.2 (br., *C*=*C*), 56.5 (d, ^2J(C,Rh) = 4.6 Hz, N−CH_2−), 47.7 (N−CH_2), 29.8 (C=C−CH_2−). − FT-IR (KBr): $\tilde{\nu}$ = 3297 (NH), 1655 (C=C), 840 $[(PF_6)^-]$, 558 $[(PF_6)^-]$. − FAB-MS (*m*/*z*): 941 $[2\ M - PF_6]^+$, 398 $[M - PF_6]^+$. − $C_{19}H_{25}F_6N_3PRh$ (543.30): calcd. C 42.00, H 4.64, N 7.73; found C 41.87, H 4.46, N 7.61.

(η^4-Cycloocta-1,5-diene)-[*N*-(2-pyridylmethyl)-*N*-(1*H*-2-pyrrolylmethyl)amine]iridium(I) Hexafluorophosphate ([2]PF_6): 77 mg (0.41 mmol) of *N*-(2-pyridylmethyl)-*N*-(1*H*-2-pyrrolylmethyl)amine (HL_H) was added to a solution of 136 mg (0.20 mmol) of

[{(cod)Ir^{I}(μ-Cl)}$_2$] in 15 mL of MeOH/CH_2Cl_2 (2:1), and stirred at room temp. for 5 min. The dichloromethane was subsequently removed from the reaction mixture under reduced pressure. After addition of 500 mg (2.7 mmol) of KPF_6 and vigorous stirring for a further 5 min, 2 mL of water was added and the reaction mixture was stored at 5°C. Yellow, X-ray quality crystals of [(HL_H)Ir^{I}-(cod)]PF_6 ([**2**]PF_6) were formed overnight. The crystals were washed with water, ethanol, and ether in order to remove the excess KPF_6. The mother liquor was treated with water to cause further precipitation of [**2**]PF_6. – ^{1}H NMR (300 MHz, CD_2Cl_2, 298 K): 9.03 (s, br., 1 H, Pyr−H1), 8.01 (m., 2 H, Py−H4 and Py−H6), 7.61 [d, 1 H, ^3J(H,H) = 7.5 Hz, Py−H3], 7.43 [dd, 1 H, ^3J(H,H) = 6.3 Hz, Py−H5], 6.77 (m., 1 H, Pyr−H5), 6.17 (m., 1 H, Pyr−H3), 6.06 (m., 1 H, Pyr−H4), 4.91 (s., br., 1 H, NH), 4.45−4.10 (m., br., 2 H, −HC=CH− and 2 H, N−CH_2−Py), 3.99 (s.,1 H, N−CH_2−Pyr), 3.97 (s., 1 H, N−CH_2−Pyr), 3.83 (br., s., 2 H, −HC=CH−) 2.28 (m., br., 4 H, −C=C−CH_2− *exo*), 1.79 (s., br., 4 H, −C=C−CH_2− *endo*). – ^{13}C{^{1}H} NMR (75 MHz, CD_2Cl_2, 298 K): δ = 163.6 (Py−C2), 148.4 (Py−C6), 141.4 (Py−C4), 125.6 (Pyr−C2), 123.8 (Py−C3), 123.7 (Py−C5), 121.0 (Pyr−C5), 112.2 (Pyr−C4), 109.3 (Pyr−C2), 68.0 (s., br., C=C), 58.5 (N−CH_2−), 50.1 (N−CH_2), 31.7 (s., br., C=C−CH_2−). – FAB-MS (*m*/*z*): 488 and 486 [M − PF_6]$^+$, 408 [M − PF_6 − CH_2 − Pyr]$^+$, 376 [M − PF_6 − (cod)]$^+$. – $C_{19}H_{25}F_6IrN_3P$ (632.59): calcd. C 36.07, H 3.98, N 6.64; found C 35.96, H 4.31, N 6.50.

(η^4-Cycloocta-1,5-diene)[(*N*-(2-pyridylmethyl)-*N*-(2-pyrrolatomethyl)amine]rhodium(I) (3): 77.6 mg (0.41 mmol) of *N*-(2-pyridylmethyl)-*N*-(1*H*-2-pyrrolylmethyl)amine (HL_H) was dissolved in 10 mL of MeOH and 100.0 mg (0.20 mmol) of [{(cod)Rh(μ-Cl)}$_2$] was added, and stirred at room temp. for 1 h. Addition of a solution of 200 mg (1.89 mmol) of Na_2CO_3 in 5 mL of water resulted in the precipitation of [(L_H^-)Rh^{I}(cod)] (**3**) as a yellow solid, which was collected by filtration, washed three times with water, once with MeOH, and vacuum dried. Crystals suitable for X-ray diffraction were obtained by slow crystallisation from a saturated toluene solution at −20°C. Yield 90 mg (56%). – ^{1}H-NMR: (200 MHz, CD_2Cl_2, 298 K): δ = 8.55 [d, 1 H, ^3J(H,H) = 4.1 Hz, Py−H6], 7.67 (m, 1 H, Py−H4), 7.21 (m, 2 H, Py−H3, Py−H5), 6.23 (s, 1 H, Pyr−H5), 5.92 [dd, 1 H, ^3J(H,H) = 2.4 Hz, ^3J(H,H) = 2.9 Hz, Pyr−H4], 5.72 [d, 1 H, ^3J(H,H) = 2.4 Hz, Pyr−H3], 4.50 (s, br, 1 H, N*H*), 4.12 (m, br, 4H −CH=CH−), 3.94 {dd[AB], 1 H, ^2J(H,H) = 14.9 Hz, ^3J(H,NH) = 3.09 Hz, N−CH_2−}, 3.81 {dd[AB], 1 H, ^2J(H,H) = 13.3 Hz, ^3J(H,NH) = 5.1 Hz, N−CH_2−}, 3.73 {dd[AB], 1 H, ^2J(H,H) = 14.9 Hz, ^3J(H,NH) = 9.9 Hz, N−CH_2−}, 3.50 {dd[AB], 1 H, ^2J(H,H) = 13.3 Hz, ^3J(H,NH) = 7.6 Hz, N−CH_2−}, 2.55 (m, 2 H, −C=C−$CH_{2\ exo}$), 2.35 (m, 2 H, −C=C−$CH_{2\ exo}$), 2.05 (m, 2 H, −C=C−$CH_{2\ endo}$), 1.85 (m, 2 H, −C=C−$CH_{2\ endo}$). – After saturation of the N−H two AB-patterns are observed for the N−CH_2− groups of the ligand: 3.93 {d[AB], 1 H, ^2J(H,H) = 14.8 Hz, N−CH}, 3.72 {d[AB], 1 H, ^2J(H,H) = 14.8 Hz, N−CH}, 3.79 {d[AB], 1 H, ^2J(H,H) = 13.1 Hz, N−CH}, 3.49 {d[AB], 1 H, ^2J(H,H) = 13.1 Hz, N−CH}. – ^{13}C NMR (50 MHz, CD_2Cl_2, 298 K): δ = 156.5 (Py−C2). 150.5 (Py−C6), 139.6 (Pyr−C2), 137.6 (Py−C4), 123.7 (Py−C3), 123.6 (Py−C5), 123.3 [d, ^2J(C,Rh) = 2.6 Hz, Pyr−C5], 108.4 (Pyr−C4), 101.7 (Pyr−C3), 79.3 [d, ^1J(C,Rh) = 12.3 Hz, C=C], 78.8 [d, ^1J(C,Rh) = 12.6 Hz, C=C], 54.0 (N−*C*H_2−Pyr), 56.1 (N−*C*H_2−Py), 32.1 (C=C−*C*H_2), 30.6 (C=C−*C*H_2). – FT-IR (KBr, cm^{-1}): $\tilde{\nu}$ = 3236 (N−H), 1654 (C=C). – FAB-MS (*m*/*z*): 398 [M + H]$^+$, 319 [M − CH_2Pyr + H]$^+$, 288 [M − cod − H]$^+$, 209 [M − cod − CH_2Pyr]$^+$. – FD$^+$-MS: 397 [M] $^+$. – $C_{19}H_{24}N_3Rh$ (397.32): calcd. C 57.44, H 6.09, N 10.58; found C 57.02, H 6.05, N 10.35.

(η^4-Cycloocta-1,5-diene)[(*N*-(2-pyridylmethyl)-*N*-(2-pyrrolatomethyl)amine]iridium(I) (4): 125 mg (0.67 mmol) of *N*-(2-pyridylmethyl)-*N*-(1*H*-2-pyrrolylmethyl)amine (HL_H) (slight xs.) was added to a suspension of 210 mg (0.31 mmol) of [{(cod)Ir^{I}(μ-Cl)}$_2$] in 15 mL of MeOH, and stirred at room temp. for 10 min. Addition of a solution of 200 mg (0.70 mmol) of $Na_2CO_3 \cdot 10\ H_2O$ in 2 mL of water resulted in the precipitation of [(L_H^-)Ir^{I}(cod)] (**4**) as a yellow solid, which was collected by filtration. Crystals suitable for X-ray diffraction were obtained by slow crystallisation from a saturated CH_2Cl_2 solution at −20°C. – ^{1}H NMR: (300 MHz, CD_2Cl_2, 298 K): δ = 8.61 [d, 1 H, ^3J(H,H) = 4.8 Hz, Py−H6], 7.70 [dd, 1 H, average ^3J(H,H) = 7.5 Hz Py−H4], 7.26 [dd, 1 H, average ^3J(H,H) = 6 Hz, Py-H5], 7.19 [d, 1 H, ^3J(H,H) = 7.5 Hz, Py−H3], 6.47 [d, 1 H, ^3J(H,H) = 2.4 Hz, Pyr−H5], 6.02 [dd, 1 H, ^3J(H,H) = 2.4 Hz], 5.86 [d, 1 H, ^3J(H,H) = 2.4 Hz, Pyr−H3], 5.25 (s., br., 1 H, N−H), 4.18 {dd[AB], 1 H, ^2J(H,H) = 15.2 Hz, ^3J(H,NH) = 2.4 Hz, N−CH}, 3.95 {dd[AB], 1 H, ^2J(H,H) = 13.4 Hz, ^3J(H,NH) = 5.3 Hz, N−CH}, 3.87 (m., 2 H −CH=CH−), 3.86 {dd[AB], 1 H, ^2J(H,H) = 15 Hz, ^3J(H,NH) = 10.2 Hz, N−CH}, 3.73 (m., 2 H, −CH=CH−), 3.58 {dd[AB], 1 H, ^2J(H,H) = 13.4 Hz, ^3J(H,NH) = 7.0 Hz, N−CH}, 2.29 (m., 2 H, −C=C−$CH_{2\ exo}$), 2.14 (m., 2 H, −C=C−$CH_{2\ exo}$), 1.82 (m., 2 H, −C=C−$CH_{2\ endo}$), 1.48 (m., 2 H, −C=C−$CH_{2\ endo}$). – ^{13}C{^{1}H} NMR (75 MHz, CD_2Cl_2, 298 K): δ = 156.2 (Py−C2). 150.6 (Py−C6), 142.0 (Pyr−C2), 137.8 (Py−C4), 123.8 (Py−C3), 123.5 (Py−C5 and Pyr−C5), 109.8 (Pyr−C4), 101.7 (Pyr−C3), 62.3 (C=C), 61.5 (C=C), 55.3 (N−*C*H_2−Pyr), 57.0 (N−*C*H_2−Py), 33.1 (C=C−*C*H_2), 31.1 (C=C−*C*H_2). – FAB-MS (*m*/*z*): 488 and 486 [M + H]$^+$, 407 [M − Py]$^+$, 376 [M − cod − H]$^+$. – $C_{19}H_{24}N_3Ir$ (486.64): calcd. C 46.90, H 4.97, N 8.63; found C 47.17, H 4.72, N 8.31.

(η^4-Cycloocta-1,5-diene)[*N*-benzyl-*N*-(2-pyridylmethyl)-*N*-(2-pyrrolatomethyl)amine]-rhodium(I) (5): To 50 mL of methanol 200 mg Na_2CO_3 (18 mmol) in 2 mL of water and 400 mg (1.449 mmol) of *N*-benzyl-*N*-(2-pyridylmethyl)-*N*-(1*H*-2-pyrrolylmethyl)amine (HL_{Bzl}) was added. The suspension was stirred for 15 min and subsequently 350 mg (0.71 mmol) of [{(cod)Rh(μ-Cl)}$_2$] was added. The mixture was stirred for 2 h at room temp. and placed at −20°C for 10 h. The resulting precipitate was collected by filtration and the yellow residue was washed three times with 5 mL of a mixture of water and MeOH (1:1), subsequently dissolved in 10 mL of CH_2Cl_2 and filtered. The yellow filtrate was evaporated under vacuum to yield [(L_{Bzl}^-)Rh^{I}(cod)] (**5**) as a yellow powder. Crystals suitable for X-ray diffraction were obtained by crystallisation from a hot saturated solution of **5** in toluene. Yield 388 mg (55%). – ^{1}H NMR (200 MHz, CD_2Cl_2, 298 K): δ = 9.25 [d, 1 H, Py−H6, ^3J(H,H) = 4.7 Hz], 7.72−7.35 (m, 6 H, Ph−H, Py−H4), 7.25 (m, 1 H, Py−H5), 7.13 [d, 1 H, ^3J(H,H) = 7.6 Hz, Py−H3], 6.34 (s, br, 1 H, Pyr−H5), 5.76 [t, 1 H, ^3J(H,H) = 2.49 Hz, Pyr−H4], 5.64 (s, br, 1 H, Pyr−H3), 4.84 {d[AB], 1 H, ^2J(H,H) = 13.7 Hz, N−CH_2−Ph}, 4.66 {d[AB], 1 H, ^2J(H,H) = 13.7 Hz, N−CH_2−Ph}, 4.01 {d[AB], 1 H, ^2J(H,H) = 14.1 Hz, N−CH_2−Py}, 4.00 {d[AB], 1 H, ^2J(H,H) = 15.0 Hz, N−CH_2−Pyr}, 3.91 (m, 2 H, −CH=CH−), 3.54 {d[AB], 1 H, ^2J(H,H) = 14.1 Hz, N−CH_2−Py}, 3.37 (m, 2 H, −CH=CH−), 3.16 {d[AB], 1 H, ^2J(H,H) = 15.0 Hz, N−CH_2−Pyr}, 2.42 (m, 4 H, C=C−$CH_{2\ exo}$), 1.73 (m, 4 H, C=C−$CH_{2\ endo}$). – ^{13}C{^{1}H} NMR (75 MHz, CD_2Cl_2, 298 K): δ = 159.0 (Py−C2), 151.7 (Py−C6), 138.3 (Pyr−C2), 137.4 (Py−C4), 135.0 (Ph−C1), 132.21 (Ph−C2), 129.1 (Ph−C3), 128.7 (Ph−C4), 125.3 (Pyr−C5), 124.1 (Py−C5), 123.8 (Py−C3), 107.3 (Pyr−C4), 103.3 (Pyr−C3), 76.0 (br., C=C), 62.5 (N−*C*H_2−Ph), 60.25 (N−*C*H_2−Pyr), 56.90 (N−*C*H_2−Py), 31.9 (C=C−*C*H_2−), 31.7 (C=C−*C*H_2−). – FAB-MS (*m*/*z*): 488 [M + H]$^+$, 409 [M − Py]$^+$, 396 [M − CH_2Py +

H]$^+$, 211 $[Rh(cod)]^+$. − $C_{26}H_{30}N_3Rh$ (487.44): calcd. C 64.07, H 6.20, N 8.62; found C 64.49, H 6.29, N 8.33.

(η⁴-Cycloocta-1,5-diene)[*N*-benzyl-*N*-(2-pyridylmethyl)-*N*-(2-pyrrolatomethyl)amine]iridium(I) (6): To a suspension of 250 mg (0.37 mmol) of $[\{(cod)Ir(\mu\text{-}Cl)\}_2]$ in 10 mL of MeOH 210 mg (0.76 mmol) of *N*-benzyl-*N*-(2-pyridylmethyl)-*N*-(1*H*-2-pyrrolylmethyl)-amine (HL_{Bzl}) was added. The reaction mixture was stirred for 15 min and subsequently 500 mg (1.75 mmol) of $Na_2CO_3 \cdot 10\,H_2O$ in 3 mL of water was added. The resulting precipitate was collected by filtration and the yellow residue was dried in vacuo to yield $[(L_{Bzl}^-)Ir^I(cod)]$ (**6**) as a yellow powder. Crystals suitable for X-ray diffraction were obtained by crystallisation from a hot saturated solution of **6** in toluene. − ^{1}H NMR (300 MHz, CD_2Cl_2, 298 K): δ = 9.24 [d, 1 H, Py−H6, ^3J(H,H) = 4.4 Hz], 7.58 [dt, 1 H, ^3J(H,H) = 7.68 Hz, J(H,H) = 1.74 Hz, Py−H4], 7.45 (m., 5 H, Ph), 7.19 [t, 1 H, average ^3J(H,H) = 6.4 Hz, Py−H5], 7.05 [d, 1 H, ^3J(H,H) = 7.8 Hz], 6.51 (m., br., 1 H, Pyr−H5), 5.78 [t, 1 H, ^3J(H,H) = 2.6 Hz, Pyr−H4], 5.73 (s., br., 1 H, Pyr−H3), 4.93 {d[AB], 1 H, ^2J(H,H) = 14.0 Hz, N−CH_2−Ph}, 4.85 {d[AB], 1 H, ^2J(H,H) = 14.0 Hz, N−CH_2−Ph}, 4.17 {d[AB], 1 H, ^2J(H,H) = 15.1 Hz, N−CH_2−Pyr}, 3.95 {d[AB], 1 H, ^2J(H,H) = 14.5 Hz, N−CH_2−Py}, 3.73 {d[AB], 1 H, ^2J(H,H) = 15.3 Hz, N−CH_2−Pyr}, 3.47 (m., 2 H, −CH=CH−), 3.03 {d[AB], 1 H, ^2J(H,H) = 14.3 Hz, N−CH_2−Py}, 2.84 (m., 2 H, −CH=CH−), 2.23 (m., 4 H, C=C−$CH_{2\,exo}$), 1.49 (m., 4 H, C=C−$CH_{2\,endo}$). − ^{13}C{^{1}H} NMR (75 MHz, CD_2Cl_2, 298 K): δ = 160.5 (Py−C2), 152.8 (Py−C6), 140.3 (Pyr−C2), 137.4 (Py−C4), 134.8 (Ph−C1), 132.1 (Ph−C2), 129.2 (Ph−C3), 129.0 (Ph−C4), 124.6 (Pyr−C5 and Py−C5), 123.3 (Py−C3), 107.6 (Pyr−C4), 102.8 (Pyr−C3), 64.0 and 62.0 (N−CH_2−Ph and N−CH_2−Pyr), 56.20 (N−CH_2−Py), 55.7 (br., C=C) 33.3 (C=C−CH_2−), 33.0 (C=C−CH_2−). − FAB-MS (*m*/*z*): 576 and 574 $[M - H]^+$, 499 $[M - Ph]^+$. $C_{26}H_{30}IrN_3$ (576.73): calcd. C 54.14, H 5.24, N 7.29; found C 54.11, H 5.08, N 7.12.

(η⁴-Cycloocta-1,5-diene)[*N*-butyl-*N*-(2-pyridylmethyl)-*N*-(2-pyrrolatomethyl)amine]rhodium(I) (7): [(*N*-Butyl-*N*-(2-pyridylmethyl)-*N*-(2-pyrrolatomethyl)amine)Rh^I(cod)] (**7**) was prepared by a method similar to the preparation of $[(L_{Bzl}^-)Rh^I(cod)]$ (**5**), starting from *N*-butyl-*N*-(2-pyridylmethyl)-*N*-(1*H*-2-pyrrolylmethyl)amine (HL_{Bu}). − ^{1}H NMR (200 MHz, $CDCl_3$, 298 K): δ = 9.10 [d, 1 H, Py−H6, ^3J(H,H) = 5.0 Hz], 7.60 (m, 1 H, Py−H4), 7.17−7.32 (m, 2 H, Py−H3, Py−H5), 6.34 (s, br, 1 H, Pyr−H5), 5.99 (m, 1 H, Pyr−H4), 5.73 (s, br, 1 H, Pyr−H3), 3.95−3.80 (m, 4 H, N−CH_2−Py, −*HC*=*CH*−), 3.75 {d[AB], 1 H, ^2J(H,H) = 13.8 Hz, N−CH_2−Pyr}, 3.51 {d[AB], 1 H, ^2J(H,H) = 14.1 Hz, N−CH_2−Pyr}, 3.40 (m, 2 H, −CH=CH−), 3.37 (m, 2 H, −CH=CH−), 3.23 [dt, 1 H, ^2J(H,H) = 12.0 Hz, ^3J(H,H) = 4.2 Hz, N−CH_2−C_3H_7], 3.04 [dt, 1 H, ^2J(H,H) = 12.0 Hz, ^3J(H,H) = 4.2 Hz, N−CH_2−C_3H_7], 2.31 (m, 4 H, C=C−$CH_{2\,exo}$), 1.88 (m, 2 H, N−CH_2−*CH_2*−C_2H_5), 1.71 (m, 4 H, C=C−$CH_{2\,endo}$), 1.40 (m, 2 H, N−C_2H_4−*CH_2*−CH_3), 0.99 [t, ^3J(H,H) = 7.2 Hz, 3 H, N−C_3H_6−*CH_3*]. − FAB-MS (*m*/*z*): 454 $[M + H]^+$, 409 $[M-Py]^+$, 375 $[M - Py]^+$, 211 $[Rh(cod)]^+$. − $C_{23}H_{32}N_3Rh$ (453.43): calcd. C 60. 79, H 7.32, N 9.25; found C 60.88, H 7.04, N 9.39.

Polymerisation of Phenylacetylene: 0.82 g of Phenylacetylene was dissolved in 20 mL of MeOH. 5 mg of catalyst $[(L_{Bzl}^-)Rh^I(cod)]$ (**5**) was added to this solution. Almost immediate formation of poly(phenylacetylene) as a yellow/orange precipitate can be observed, and a gradual colour change of the solution from pale yellow to deep red. After 20 min the poly(phenylacetylene) precipitate was collected by filtration, washed with MeOH and dried under vacuum. Yield 0.20 g (24%). − IR (KBr): ṽ = 3053, 1596, 1488, 1444, 1073, 1028, 884, 756, 737, 696 cm^{-1}. − ^{1}H NMR (200 MHz, $CDCl_3$, 298 K): δ = 6.98 (s, br. Ph), 6.67 (m, br., Ph), 5.86 (s, br., vinyl). − GPC analysis (polystyrene standard): M_n = 14000, M_w = 65000, M_z = 137000, M_w/M_n = 4.7, M_z/M_w = 2.1, $[\eta]_{dv}$ = 0.292.

Acknowledgments

We thank Roel Fokkens of the University of Amsterdam for performing high resolution MS- measurements. We thank Johnson Matthey Ltd. for a generous loan of $RhCl_3 \cdot 3\,H_2O$ and $IrCl_3 \cdot 3\,H_2O$.

[1] $[(Cn^*)Rh^{III}(Me)]^+$ is active in polymerisation of ethene: [1a] L. Wang, T. C. Flood, *J. Am. Chem. Soc*. **1992**, *114*, 3169. − [1b] L. Wang, R. S. Lu, R. Bau, T. C. Flood, *J. Am. Chem. Soc*. **1993**, *115*, 6999.

[2] $[(Cn^*)Rh^I(PMe_3)]^+$ and $[(Tp^{Me2})Rh^I(CO)]$ oxidatively add C−H bonds: [2a] C. Wang, J. W. Ziller, T. C. Flood, *J. Am. Chem. Soc*. **1995**, *117*, 1647. − [2b] C. K. Ghosh, W. A. G. Graham, *J. Am. Chem. Soc*. **1987**, *109*, 4726. − [2c] C. K. Ghosh, W. A. G. Graham, *J. Am. Chem. Soc*. **1989**, *111*, 375. − [2d] P. E. Bloyce, J. Mascetti, A. J. Rest, *J. Organomet. Chem.* **1993**, *444*, 223. − [2e] A. A. Purwoko, A. J. Lees, *Inorg. Chem.* **1996**, *35*, 675.

[3] The α-chlorotolyl complex $[(2,6\text{-}(C(Me)=N-i\text{Pr})_2C_5H_3N)Rh^{II}Cl_2(CHClPh)]$ reacts with H_2O and O_2 to give benzaldehyde and H_2O_2: H. F. Haarman, F. R. Bregman, P. W. N. M. van Leeuwen, K. Vrieze, *Organometallics* **1997**, *16*, 979.

[4] B. de Bruin, M. J. Boerakker, J. J. J. M. Donners, B. E. C. Christiaans, P. P. J. Schlebos, R. de Gelder, J. M. M. Smits, A. L. Spek, A. W. Gal, *Angew. Chem*. **1997**, *109*, 2153; *Angew. Chem. Int. Ed. Eng*. **1997**, *36*, 2064.

[5] [5a] M. A. Esteruelas, F. J. Lahoz, A. M. Lopez, E. Onate, L. A. Oro, N. Ruiz, E. Sola, J. I. Tolosa, *Inorg. Chem.* **1996**, *35*, 7811. − [5b] P. G. Rasmussen, O. H. Bailey, J. C. Bayon, *Inorg. Chem*. **1984**, *23*, 343. − [5c] S. W. Kaiser, R. B. Saillant, W.M. Butler, P.G. Butler, P.G. Rasmussen, *Inorg. Chem*. **1976**, *15*, 2681. − [5d] M. Akita, K. Ohta, Y. Takahashi, S. Hikichi, Y. Moro-oka, *Organometallics* **1997**, *16*, 4121. − [5e] M. Bortolin, U. E. Bucher, H. Rüegger, L. M. Venanzi, A. Albinati, F. Lianza, S. Trofimenko, *Organometallics* **1992**, *11*, 2514. − [5f] H. Brunner, P. Beier, G. Riepl, I. Bernal, G. M. Reisner, R. Benn, A. Rufinska, *Organometallics* **1985**, *4*, 1732. − [5g] K. A. Beveridge, G. W. Bushnell, S. R. Stobart, J. L. Atwood, M. J. Zaworotko, *Organometallics* **1983**, *2*, 1447. − [5h] M. Cocivera, G. Ferguson, B. Kaitner, F. J. Lalor, D. J. O′Sullivan, M. Pavez, B. Ruhl, *Organometallics* **1982**, *1*, 1132. − [5i] M. A. Garalda, R. Hernandez, L. Ibarlucea, M. I. Arriotua, M. K. Urtiaga, *Inorg. Chim. Acta* **1995**, *232*, 9. − [5j] H. Brunner, G. Riepl, I. Bernal, W. H. Ries, *Inorg. Chim. Acta* **1986**, *112*, 65. − [5k] M. P. Garcia, A. M. Lopez, M. A. Esteruelas, F. J. Lahoz, L. A. Oro, *J. Chem. Soc., Chem. Comm.* **1988**, 793. − [5l] K. Yamamoto, H. Tateishi, W. Watanabe, T. Adachi, H. Matsubara, T. Ueda, T. Yoshida, *J. Chem. Soc., Chem. Comm* **1995**, 1637. − [5m] F. J. Lahoz, A. Tiripicchio, M. Tiripicchio Camellini, L. A. Oro, M. T. Pinillos, *J. Chem. Soc., Dalton Trans.* **1985**, 1487. − [5n] D. Sanz, M. D. Santa Maria, R. M. Claramunt, M. Cano, J. V. Heras, J. A. Campo, F. A. Ruiz, E. Pinilla, A. Monge, *J. Organomet. Chem*. **1996**, *523*, 179. − [5o] H. Brunner, B. Nubber, M. Prommesberger, *J. Organomet. Chem.* **1996**, *526*, 341. − [5p] W. S. Sheldrick, B. Gunther, *J. Organomet. Chem.* **1991**, *402*, 256. − [5q] W. S. Sheldrick, B. Gunther, *J. Organomet. Chem.* **1989**, *375*, 233. − [5r] A. Albinati, C. Arz, P. S. Preggosin, *J. Organomet. Chem*. **1988**, *356*, 367. − [5s] M. A. Esteruelas, L. A. Oro, M. C. Apreda, C. Foces-Foces, F. H. Cano, R. M. Claramunt, C. Lopez, J. Elguero, M. Begtrup, *J. Organomet. Chem*. **1988**, *344*, 93. − [5t] L. A. Oro, M Esteban, R. M. Claramunt, J. Elguero, C. Foces-Foces, F. H. Cano, *J. Organomet. Chem*. **1984**, 276, 79. − [5u] B.M Louie, S. J. Rettig, A. Storr, J. Trotter, *Can. J. Chem*. **1984**, *62*, 1057. − [5v] W. H. Watson, A. Nagl, A. P. Marchand, P. Annapurna, *Acta Crystallogr., Sect. C (Cr. Str. Comm.)* **1989**, *45*, 856.

[6] [6a] H. M. Colquhoun, S. M. Doughty, J. F. Stoddart, D. J. Williams, *J. Chem. Soc., Dalton Trans.* **1986**, 1639. − [6b] A. A. H.

van der Zeijden, G. Van Koten, R. A. Nordemann, B. Kojic-Prodic, A. L. Spek, *Organometallics* **1988**, *7*, 1957.
[7] A. R. Rossi, R. Hoffmann, *Inorg. Chem.* **1975**, *14* (2), 365.
[8] [8a] G. Winkhaus, H. Singer, *Chem. Ber.* **1966**, *99*, 3610. – [8b] G. Mestroni, A. Camus, G. Zassinovich, *J. Organomet. Chem.* **1974**, *73*, 119. – [8c] M. A. Esteruelas, L. A. Oro, M. C. Apreda, C. Foces-Foces, F. H. Cano, R. M. Claramunt, C. Lopex, J. Elguero, M. Bergtrup, *J. Organomet. Chem.* **1988**, *344*, 93.
[9] H Katayama, K. Yamamura, Y. Miyaki, F. Ozawa, *Organometallics* **1997**, *16*, 4497.
[10] [10a] Y. Kishimoto, P. Eckerle, T. Miyatake, T. Ikariya, R Noyori, *J. Am. Chem. Soc.* **1994**, *116*, 12131. – [10b] A. Escudero, R. Vilar, R. Salcedo, T. Ogawa, *Eur. Polym. J.* **1995**, *11*, 1135 and references quoted therein.
[11] [11a] S. Trofimenko, *Chem. Rev.* **1993**, *93*, 943. – [11b] N. Kitajima, W. B. Tolman, *Prog. Inorg. Chem.* **1995**, *43*, 419.
[12] Diene complexes: [12a] M. Akita, K. Ohta, Y. Takahashi, S. Hikichi, Y. Moro-oka, *Organometallics* **1997**, *16*, 4121. – [12b] M. Cocivera, T. J. Desmond, G. Ferguson, B. Kaitner, F. J. Lalor, D. J. O′Sullivan, *Organometallics* **1982**, *1*, 1125. – [12c] M. Cocivera, G. Ferguson, B. Kaitner, F. J. Lalor, D. J. O′Sullivan, M. Pavez, B. Ruhl, *Organometallics* **1982**, *1*, 1132. – [12d] M. Cocivera, G. Ferguson, F. J. Lalor, P. Szczecinski, *Organometallics* **1982**, *1*, 1139. – [12e] U. E. Bucher, A. Currao, R. Nesper, H. Rüegger, L. M. Venanzi, E. Younger, *Inorg. Chem.* **1995**, *34*, 66. – [12f] U. E. Bucher, T. F. Fässler, M. Hunziker, R. Nesper, H. Rüegger, L. M. Venanzi, *Gazz. Chim. Ital.* **1995**, *125*, 181. – [12g] D. Sanz, M. D. Santa Maria, R. M. Claramunt, M. Cano, J. V. Heras, J. A. Campo, F. A. Ruiz, E. Pinilla, A. Monge, *J. Organomet. Chem.* **1996**, *523*, 179.
[13] Olefin complexes: [13a] S. Trofimenko, *J. Am. Chem. Soc.* **1969**, *91*, 588. – [13b] W. J. Oldham, D. M. Heinekey, *Organometallics* **1997**, *16*, 467. – [13c] P. J. Pérez, M. L. Poveda, E. Carmona, *Angew. Chem. Int. Ed Engl.* **1995**, *34*, 66.
[14] G. Giordano, R. H. Crabtree, *Inorg. Synth.* **1990**, *28*, 88.
[15] J. L. Herde, J. C. Lambert, C. V. Senov, *Inorg. Synth.* **1974**, XV, 18.
[16] A. C. T. North, D. C. Phillips, F. C. Mathews, *Acta Cryst.* **1968**, *A24*, 351.
[17] P. T. Beurskens, G. Beurskens, W. P. Bosman, R. de Gelder, S. Garcia-Granda, R. O. Gould, R. Israel, J. M. M. Smits. *DIRDIF-96*. A computer program system for crystal structure determination by Patterson methods and direct methods applied to difference structure factors; Laboratory of Crystallography, Department of Inorganic Chemistry, University of Nijmegen: The Netherlands, **1996**.
[18] P. T. Beurskens, G. Beurskens, M. Strumpel, C. E. Nordman. In: *Patterson and Pattersons* (Eds.: J. P. Glusker, B. K. Patterson, M. Rossi); Clarendon Press: Oxford, **1987**; p. 356.
[19] R. de Gelder, R. A. G. de Graaff, H. Schenk, *Acta Cryst.* **1993**, A49, 297.
[20] G. M. Sheldrick, *SHELXL-97*. Program for the refinement of crystal structures; University of Göttingen: Germany, **1997**.

Received March 8, 1999
[I99095]